



1
2
3 **Mitochondrial respiratory states and rates:**
4 **Building blocks of mitochondrial physiology Part 1**

5
6 **COST Action CA15203 MitoEAGLE preprint** Version: 2018-10-16(43)

7
8 Corresponding author: Gnaiger E

9 Co-authors:

10 Aasander Frostner E, Abumrad NA, Acuna-Castroviejo D, Adams SH, Ahn B, Ali SS, Alves MG,
11 Amati F, Amoedo ND, Aral C, Arandarčikaitė O, Arnould T, Avram VF, Bailey DM, Bajpeyi S,
12 Bakker BM, Bastos Sant'Anna Silva AC, Battino M, Bazil J, Beard DA, Bednarczyk P, Bello F, Ben-
13 Shachar D, Bergdahl A, Berge RK, Bernardi P, Bishop D, Blier PU, Blindheim DF, Boetker HE,
14 Boros M, Borsheim E, Borutaitė V, Bouillaud F, Bouitbir J, Boushel RC, Bovard J, Breton S, Brown
15 DA, Brown GC, Brown RA, Brozinick JT, Buettner GR, Burtscher J, Calabria E, Calbet JA, Calzia E,
16 Cannon DT, Cano Sanchez M, Canto AC, Cardoso LHD, Carvalho E, Casado Pinna M, Cassina AM,
17 Castro L, Cavalcanti-de-Albuquerque JP, Cervinkova Z, Chabi B, Chakrabarti L, Chaurasia B, Chen
18 Q, Chicco AJ, Chinopoulos C, Chowdhury SK, Cizmarova B, Clementi E, Coen PM, Coker RH,
19 Collin A, Crisóstomo L, Dambrova M, Danhelovska T, Darveau CA, Das AM, Dash RK, Davidova E,
20 Davis MS, De Goede P, De Palma C, Dembinska-Kiec A, Devaux Y, Di Marcello M, Dias TR,
21 Distefano G, Doermann N, Doerrier C, Donnelly C, Drahota Z, Dubouchaud H, Duchon MR, Dumas
22 JF, Durham WJ, Dymkowska D, Dyrstad SE, Dyson A, Dzialowski EM, Ehinger J, Elmer E,
23 Endlicher R, Engin AB, Escames G, Ezrova Z, Falk MJ, Fell DA, Ferko M, Ferreira JCB, Ferreira R,
24 Fessel JP, Filipovska A, Fisar Z, Fischer M, Fisher G, Fisher JJ, Ford E, Fornaro M, Galina A, Galkin
25 A, Galli GL, Gan Z, Ganetzky R, Garcia-Roves PM, Garcia-Souza LF, Garipi E, Garlid KD, Garrabou
26 G, Garten A, Gastaldelli A, Genova ML, Giovarelli M, Gonzalez-Armenta JL, Gonzalo H, Goodpaster
27 BH, Gorr TA, Gourlay CW, Granata C, Grefte S, Guarch ME, Gueguen N, Gumeni S, Haas CB,
28 Haavik J, Haendeler J, Hamann A, Han J, Han WH, Hancock CR, Hand SC, Hargreaves IP, Harrison
29 DK, Heales SJR, Hellgren KT, Hepple RT, Hernansanz-Agustin P, Hickey AJ, Hoel F, Holland OJ,
30 Holloway GP, Hoppel CL, Hoppel F, Houstek J, Huete-Ortega M, Iglesias-Gonzalez J, Irving BA,
31 Iyer S, Jackson CB, Jadiya P, Jang DH, Jang YC, Janowska J, Jansen-Dürr P, Jansone B,
32 Jarmuszkiewicz W, Jespersen NR, Jha RK, Jurczak MJ, Jurk D, Kaambre T, Kaczor JJ, Kainulainen
33 H, Kandel SM, Kane DA, Kappler L, Karabatsiakakis A, Karkucinska-Wieckowska A, Keijer J, Keller
34 MA, Keppner G, Khamoui AV, Kilbaugh T, Klepinin A, Klingenspor M, Komlodi T, Koopman WJH,
35 Kopitar-Jerala N, Kowaltowski AJ, Kozlov AV, Krajcova A, Krako Jakovljevic N, Kristal BS, Kuang
36 J, Kucera O, Kuka J, Kwak HB, Kwast K, Laasmaa M, Labieniec-Watala M, Lai N, Land JM, Lane N,
37 Laner V, Lanza IR, Larsen TS, Lavery GG, Lee HK, Leeuwenburgh C, Lemieux H, Lenaz G, Lerfall
38 J, Li PA, Liepins E, Liu J, Lucchinetti E, Macedo MP, MacMillan-Crow LA, Makarova E, Makrečka-
39 Kuka M, Malik A, Markova M, Martin DS, Mazat JP, McKenna HT, Menze MA, Merz T, Meszaros
40 AT, Methner A, Michalak S, Moellering DR, Moiso N, Molina AJA, Montaigne D, Moore AL,
41 Moreau K, Moreno-Sánchez R, Moreira BP, Mracek T, Muntane J, Muntean DM, Murray AJ, Nair
42 KS, Nehlin JO, Nemeč M, Neuffer PD, Neuzil J, Neviere R, Newsom S, Nozickova K, O'Brien KA,
43 O'Gorman D, Olgar Y, Oliveira MF, Oliveira MT, Oliveira PF, Oliveira PJ, Orynbayeva Z, Osiewacz
44 HD, Ounpuu L, Pak YK, Pallotta ML, Palmeira CM, Parajuli N, Passos JF, Passrugger M, Patel HH,
45 Pavlova N, Pecina P, Pelena D, Pereira da Silva Grilo da Silva F, Perez Valencia JA, Pesta D, Petit
46 PX, Pettersen IKN, Pichaud N, Piel S, Pietka TA, Pino MF, Pirkmajer S, Porter C, Porter RK, Pranger
47 F, Prochownik EV, Pulinilkunnil T, Puskarich MA, Puurand M, Quijano C, Radenkovic F, Radi R,
48 Ramzan R, Rattan S, Reboredo P, Rich PR, Renner-Sattler K, Rial E, Robinson MM, Roden M,

49 Rodríguez-Enriquez S, Rohlena J, Rolo AP, Ropelle ER, Røslund GV, Rossignol R, Rossiter HB,
50 Rubelj I, Rybacka-Mossakowska J, Saada A, Safaei Z, Salin K, Salvadego D, Sandi C, Sanz A,
51 Sazanov LA, Scatena R, Schartner M, Scheibye-Knudsen M, Schilling JM, Schlattner U, Schönfeld P,
52 Schwarzer C, Scott GR, Shabalina IG, Sharma P, Sharma V, Shevchuk I, Siewiera K, Silber AM,
53 Silva AM, Sims CA, Singer D, Skolik R, Smenes BT, Smith J, Soares FAA, Sobotka O, Sokolova I,
54 Sonkar VK, Sowton AP, Sparagna GC, Sparks LM, Spinazzi M, Stankova P, Starr J, Stary C, Stelfa
55 G, Stiban J, Stier A, Stocker R, Sumbalova Z, Suravajhala P, Swerdlow RH, Swiniuch D, Szabo I,
56 Szewczyk A, Szibor M, Tanaka M, Tandler B, Tarnopolsky MA, Tausan D, Tavernarakis N, Tepp K,
57 Thyfault JP, Tomar D, Towheed A, Tretter L, Trifunovic A, Trivigno C, Tronstad KJ, Trougakos IP,
58 Tuncay E, Turan B, Tyrrell DJ, Urban T, Valentine JM, Vendelin M, Vercesi AE, Victor VM, Viel C,
59 Vieyra A, Vilks K, Villena JA, Vinogradov AD, Viscomi C, Vitorino RMP, Vogt S, Volani C, Volska
60 K, Votion DM, Vujacic-Mirski K, Wagner BA, Ward ML, Warnsmann V, Wasserman DH, Watala C,
61 Wei YH, Wickert A, Wieckowski MR, Williams C, Winwood-Smith H, Wohlgemuth SE, Wohlwend
62 M, Wolff J, Wüst RCI, Yokota T, Zablocki K, Zaugg K, Zaugg M, Zdrzilova L, Zhang Y, Zhang YZ,
63 Zíková A, Zischka H, Zorzano A, Zvejniece L
64

65 **Updates and discussion:**

66 http://www.mitoeagle.org/index.php/MitoEAGLE_preprint_2018-02-08
67

68 Correspondence: Gnaiger E

69 *Chair COST Action CA15203 MitoEAGLE* – <http://www.mitoeagle.org>

70 *Department of Visceral, Transplant and Thoracic Surgery, D. Swarovski Research Laboratory,*

71 *Medical University of Innsbruck, Innrain 66/4, A-6020 Innsbruck, Austria*

72 *Email: mitoeagle@i-med.ac.at; Tel: +43 512 566796, Fax: +43 512 566796 20*
73

| | |
|-----|---|
| 74 | Table of contents |
| 75 | |
| 76 | Abstract |
| 77 | Executive summary |
| 78 | 1. Introduction – Box 1: In brief: Mitochondria and Bioblasts |
| 79 | 2. Coupling states and rates in mitochondrial preparations |
| 80 | 2.1. <i>Cellular and mitochondrial respiration</i> |
| 81 | 2.1.1. Aerobic and anaerobic catabolism and ATP turnover |
| 82 | 2.1.2. Specification of biochemical dose |
| 83 | 2.2. <i>Mitochondrial preparations</i> |
| 84 | 2.3. <i>Electron transfer pathways</i> |
| 85 | 2.4. <i>Respiratory coupling control</i> |
| 86 | 2.4.1. Coupling |
| 87 | 2.4.2. Phosphorylation, P _s , and P _s /O ₂ ratio |
| 88 | 2.4.3. Uncoupling |
| 89 | 2.5. <i>Coupling states and respiratory rates</i> |
| 90 | 2.5.1. LEAK-state |
| 91 | 2.5.2. OXPHOS-state |
| 92 | 2.5.3. Electron transfer-state |
| 93 | 2.5.4. ROX state and <i>Rox</i> |
| 94 | 2.5.5. Quantitative relations |
| 95 | 2.5.6. The steady-state |
| 96 | 2.6. <i>Classical terminology for isolated mitochondria</i> |
| 97 | 2.6.1. State 1 |
| 98 | 2.6.2. State 2 |
| 99 | 2.6.3. State 3 |
| 100 | 2.6.4. State 4 |
| 101 | 2.6.5. State 5 |
| 102 | 2.7. <i>Control and regulation</i> |
| 103 | 3. What is a rate? – Box 2: Metabolic flows and fluxes: vectorial, vectorial, and scalar |
| 104 | 4. Normalization of rate per sample |
| 105 | 4.1. <i>Flow: per object</i> |
| 106 | 4.1.1. Number concentration |
| 107 | 4.1.2. Flow per object |
| 108 | 4.2. <i>Size-specific flux: per sample size</i> |
| 109 | 4.2.1. Sample concentration |
| 110 | 4.2.2. Size-specific flux |
| 111 | 4.3. <i>Marker-specific flux: per mitochondrial content</i> |
| 112 | 4.3.1. Mitochondrial concentration and mitochondrial markers |
| 113 | 4.3.2. mt-Marker-specific flux |
| 114 | 5. Normalization of rate per system |
| 115 | 5.1. <i>Flow: per chamber</i> |
| 116 | 5.2. <i>Flux: per chamber volume</i> |
| 117 | 5.2.1. System-specific flux |
| 118 | 5.2.2. Advancement per volume |
| 119 | 6. Conversion of units |
| 120 | 7. Conclusions – Box 3: Recommendations for studies with mitochondrial preparations |
| 121 | References |
| 122 | Supplement |
| 123 | S1. Manuscript phases and versions - an open-access approach |
| 124 | S2. Authors |
| 125 | |

126 **Abstract** As the knowledge base and importance of mitochondrial physiology to human health expands,
 127 the necessity for harmonizing the terminology concerning mitochondrial respiratory states and rates has
 128 become increasingly apparent. The chemiosmotic theory establishes the mechanism of energy
 129 transformation and coupling in oxidative phosphorylation. The unifying concept of the protonmotive
 130 force provides the framework for developing a consistent theoretical foundation of mitochondrial
 131 physiology and bioenergetics. We follow IUPAC guidelines on terminology in physical chemistry,
 132 extended by considerations on open systems and thermodynamics of irreversible processes. The
 133 concept-driven constructive terminology incorporates the meaning of each quantity and aligns concepts
 134 and symbols to the nomenclature of classical bioenergetics. We endeavour to provide a balanced view
 135 on mitochondrial respiratory control and a critical discussion on reporting data of mitochondrial
 136 respiration in terms of metabolic flows and fluxes. Uniform standards for evaluation of respiratory states
 137 and rates will ultimately contribute to reproducibility between laboratories and thus support the
 138 development of databases of mitochondrial respiratory function in species, tissues, and cells. Clarity of
 139 concept and consistency of nomenclature facilitate effective transdisciplinary communication,
 140 education, and ultimately further discovery.

141
 142 *Keywords:* Mitochondrial respiratory control, coupling control, mitochondrial preparations,
 143 protonmotive force, uncoupling, oxidative phosphorylation, OXPHOS, efficiency, electron transfer, ET;
 144 electron transfer system, ETS; proton leak, LEAK, residual oxygen consumption, ROX, State 2, State
 145 3, State 4, normalization, flow, flux, O₂
 146

147 **Executive summary**

148
 149 In view of the broad implications for health care, mitochondrial researchers face an increasing
 150 responsibility to disseminate their fundamental knowledge and novel discoveries to a wide range of
 151 stakeholders and scientists beyond the group of specialists. This requires implementation of a commonly
 152 accepted terminology within the discipline and standardization in the translational context. Authors,
 153 reviewers, journal editors, and lecturers are challenged to collaborate with the aim to harmonize the
 154 nomenclature in the growing field of mitochondrial physiology and bioenergetics, from evolutionary
 155 biology and comparative physiology to mitochondrial medicine. In the present communication we focus
 156 on the following concepts in mitochondrial physiology:

- 157 1. Aerobic respiration depends on the coupling of phosphorylation (ADP → ATP) to O₂ flux in
 158 catabolic reactions. Coupling in oxidative phosphorylation is mediated by the translocation of
 159 protons across the inner mitochondrial membrane through proton pumps generating or
 160 utilizing the protonmotive force, that is maintained between the mitochondrial matrix and
 161 intermembrane compartment or outer mitochondrial space. Compartmental coupling
 162 distinguishes this vectorial component of oxidative phosphorylation from glycolytic
 163 fermentation as the counterpart of cellular core energy metabolism (**Figure 1**). Cell respiration
 164 is distinguished from fermentation: (1) Electron acceptors are supplied by external respiration
 165 for the maintenance of redox balance, whereas fermentation is characterized by an internal
 166 electron acceptor produced in intermediary metabolism. In aerobic cell respiration, redox
 167 balance is maintained by O₂ as the electron acceptor. (2) Compartmental coupling in vectorial
 168 oxidative phosphorylation contrasts to exclusively scalar substrate-level phosphorylation in
 169 fermentation.
- 170 2. When measuring mitochondrial metabolism, the contribution of fermentation and other cytosolic
 171 interactions must be excluded from analysis by disrupting the barrier function of the plasma
 172 membrane. Selective removal or permeabilization of the plasma membrane yields
 173 mitochondrial preparations—including isolated mitochondria, tissue and cellular
 174 preparations—with structural and functional integrity. Subsequently, extra-mitochondrial
 175 concentrations of fuel substrates, ADP, ATP, inorganic phosphate, and cations including H⁺
 176 can be controlled to determine mitochondrial function under a set of conditions defined as
 177 *coupling control states*. We strive to incorporate an easily recognized and understood, concept-
 178 driven terminology of bioenergetics with explicit terms and symbols that define the nature of
 179 respiratory states.
- 180 3. Mitochondrial coupling states are defined according to the control of respiratory oxygen flux by
 181 the protonmotive force. Capacities of oxidative phosphorylation and electron transfer are

measured at kinetically saturating concentrations of fuel substrates, ADP and inorganic phosphate, and O₂, or at optimal uncoupler concentrations, respectively, in the absence of Complex IV inhibitors such as NO, CO, or H₂S. Respiratory capacity is a measure of the upper bound of the rate of respiration; it depends on the substrate type undergoing oxidation, and provides reference values for the diagnosis of health and disease, and for evaluation of the effects of Evolutionary background, Age, Gender and sex, Lifestyle and Environment.

Figure 1. Internal and external respiration

Mitochondrial respiration is the oxidation of fuel substrates (electron donors) and reduction of O₂ catalysed by the electron transfer system, ETS: (mt) mitochondrial catabolic respiration; (ce) total cellular O₂ consumption; and (ext) external respiration. All chemical reactions, r , that consume O₂ in the cells of an organism, contribute to cell respiration, J_{rO_2} . In addition to mitochondrial catabolic respiration, O₂ is consumed by:

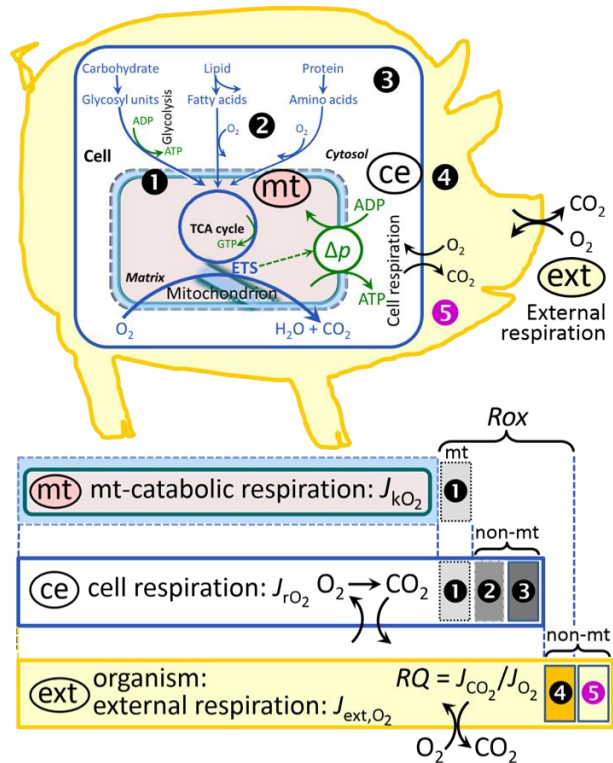
- 1 Mitochondrial residual O₂ consumption, R_{ox} .
- 2 Non-mitochondrial O₂ consumption by catabolic reactions, particularly peroxisomal oxidases and microsomal cytochrome P450 systems.
- 3 Non-mitochondrial R_{ox} by reactions unrelated to catabolism.
- 4 Extracellular mt- R_{ox} and non-mt R_{ox} are measured without fuel substrate supply or after inhibiting the ETS.
- 5 Aerobic microbial respiration.

(mt) **Mitochondrial catabolic respiration**, J_{kO_2} , is the O₂ consumption by the mitochondrial ETS excluding R_{ox} .

(ce) **Cell respiration**, J_{rO_2} , takes into account internal O₂-consuming reactions, r , including catabolic respiration and R_{ox} . Catabolic cell respiration is the O₂ consumption associated with catabolic pathways in the cell, including mitochondrial catabolism in addition to peroxisomal and microsomal oxidation reactions (2).

(ext) **External respiration** balances internal respiration at steady-state, including extracellular R_{ox} (4) and aerobic respiration by the microbiome (5). O₂ is transported from the environment across the respiratory cascade, *i.e.*, circulation between tissues and diffusion across cell membranes, to the intracellular compartment. The respiratory quotient, RQ , is the molar CO₂/O₂ exchange ratio; when combined with the respiratory nitrogen quotient, N/O₂ (mol N given off per mol O₂ consumed), the RQ reflects the proportion of carbohydrate, lipid and protein utilized in cell respiration during aerobically balanced steady-states. Bicarbonate and CO₂ are transported in reverse to the extracellular milieu and the organismic environment. Hemoglobin provides the molecular paradigm for the combination of O₂ and CO₂ exchange, as do lungs and gills on the morphological level.

4. Incomplete tightness of coupling, *i.e.*, some degree of uncoupling relative to the substrate-dependent coupling stoichiometry, is a characteristic of energy-transformations across membranes. Uncoupling is caused by a variety of physiological, pathological, toxicological, pharmacological and environmental conditions that exert an influence not only on the proton leak and cation cycling, but also on proton slip within the proton pumps and the structural integrity of the mitochondria. A more loosely coupled state is induced by stimulation of mitochondrial superoxide formation and the bypass of proton pumps. In addition, the use of protonophores represents an experimental uncoupling intervention to assess the transition from a well-coupled to a noncoupled state of mitochondrial respiration.
5. Respiratory oxygen consumption rates have to be carefully normalized to enable meta-analytic studies beyond the question of a particular experiment. Therefore, all raw data on rates and



238 variables for normalization should be published in an open access data repository.
 239 Normalization of rates for: (1) the number of objects (cells, organisms); (2) the volume or
 240 mass of the experimental sample; and (3) the concentration of mitochondrial markers in the
 241 experimental chamber are sample-specific normalizations, which are distinguished from
 242 system-specific normalization for the volume of the chamber (the measuring system).

243 6. The consistent use of terms and symbols will facilitate transdisciplinary communication and
 244 support the further development of a collaborative database on bioenergetics and
 245 mitochondrial physiology. The present considerations are focused on studies with
 246 mitochondrial preparations. These will be extended in a series of reports on pathway control
 247 of mitochondrial respiration, respiratory states in intact cells, and harmonization of
 248 experimental procedures.
 249

250 **Box 1: In brief – Mitochondria and Bioblasts**

251 *‘For the physiologist, mitochondria afforded the first opportunity for an experimental*
 252 *approach to structure-function relationships, in particular those involved in active*
 253 *transport, vectorial metabolism, and metabolic control mechanisms on a subcellular level’*
 254 (Ernster and Schatz 1981).

255 Mitochondria are oxygen-consuming electrochemical generators that evolved from the endosymbiotic
 256 alphaproteobacteria which integrated into a host cell related to Asgard Archaea (Margulis 1970; Lane
 257 2005; Roger *et al.* 2017). They were described by Richard Altmann (1894) as ‘bioblasts’, which include
 258 not only the mitochondria as presently defined, but also symbiotic and free-living bacteria. The word
 259 ‘mitochondria’ (Greek mitos: thread; chondros: granule) was introduced by Carl Benda (1898).

260 Contrary to current textbook dogma, mitochondria form dynamic networks within eukaryotic
 261 cells. Mitochondrial movement is supported by microtubules and morphology can change in response
 262 to energy requirements of the cell via processes known as fusion and fission; these interactions allow
 263 mitochondria to communicate within a network (Chan 2006). Mitochondria can even traverse cell
 264 boundaries in a process known as horizontal mitochondrial transfer (Torralba *et al.* 2016). Another
 265 defining characteristic of mitochondria is the double membrane. The mitochondrial inner membrane
 266 (mtIM) forms dynamic tubular to disk-shaped cristae that separate the mitochondrial matrix, *i.e.*, the
 267 negatively charged internal mitochondrial compartment, from the intermembrane space; the latter being
 268 enclosed by the mitochondrial outer membrane (mtOM) and positively charged with respect to the
 269 matrix. The mtIM contains the non-bilayer phospholipid cardiolipin, which is not present in any other
 270 eukaryotic cellular membrane. Cardiolipin has many regulatory functions (Oemer *et al.* 2018); in
 271 particular, it stabilizes and promotes the formation of respiratory supercomplexes (SC I_nIII_nIV_n), which
 272 are supramolecular assemblies based upon specific and dynamic interactions between individual
 273 respiratory complexes (Greggio *et al.* 2017; Lenaz *et al.* 2017). The fluidity of the mitochondrial
 274 membrane is plastic and exerts an influence on the functional properties of proteins incorporated in
 275 membranes (Waczulikova *et al.* 2007). Intracellular stress factors may cause shrinking or swelling of
 276 the mitochondrial matrix, that can ultimately result in permeability transition.

277 Mitochondria are the structural and functional elementary components of cell respiration.
 278 Mitochondrial respiration is the reduction of molecular oxygen by electron transfer coupled to
 279 electrochemical proton translocation across the mtIM. In the process of oxidative phosphorylation
 280 (OXPHOS), the catabolic reaction of oxygen consumption is electrochemically coupled to the
 281 transformation of energy in the form of adenosine triphosphate (ATP; Mitchell 1961, 2011).
 282 Mitochondria are the powerhouses of the cell which contain the machinery of the OXPHOS-pathways,
 283 including transmembrane respiratory complexes (proton pumps with FMN, Fe-S and cytochrome *b*, *c*,
 284 *aa*₃ redox systems); alternative dehydrogenases and oxidases; the coenzyme ubiquinone (Q); F-ATPase
 285 or ATP synthase; the enzymes of the tricarboxylic acid cycle (TCA), fatty acid and amino acid oxidation;
 286 transporters of ions, metabolites and co-factors; iron/sulphur cluster synthesis; and mitochondrial
 287 kinases related to catabolic pathways. The mitochondrial proteome comprises over 1,200 proteins
 288 (Calvo *et al.* 2015; 2017), mostly encoded by nuclear DNA (nDNA), with a variety of functions, many
 289 of which are relatively well known (*e.g.*, proteins regulating mitochondrial biogenesis or apoptosis),
 290 while others are still under investigation, or need to be identified (*e.g.*, permeability transition pore,
 291 alanine transporter). Only recently has it been possible to use the mammalian mitochondrial proteome
 292 to discover and characterize the genetic basis of mitochondrial diseases (Williams *et al.* 2016; Palmfeldt
 293 and Bross 2017).

294 Numerous cellular processes are orchestrated by a constant crosstalk between mitochondria and
295 other cellular components. For example, the crosstalk between mitochondria and the endoplasmic
296 reticulum is involved in the regulation of calcium homeostasis, cell division, autophagy, differentiation,
297 and anti-viral signaling (Murley and Nunnari 2016). Mitochondria contribute to the formation of
298 peroxisomes, which are hybrids of mitochondrial and ER-derived precursors (Sugiura *et al.* 2017).
299 Cellular mitochondrial homeostasis (mitostasis) is maintained through regulation at transcriptional,
300 post-translational and epigenetic levels. Cell signalling modules contribute to homeostatic regulation
301 throughout the cell cycle or even cell death by activating proteostatic modules (*e.g.*, the ubiquitin-
302 proteasome and autophagy-lysosome/vacuole pathways; specific proteases like LON) and genome
303 stability modules in response to varying energy demands and stress cues (Quiros *et al.* 2016). Several
304 post-translational modifications, including acetylation and nitrosylation, are also capable of influencing
305 the bioenergetic response, with clinically significant implications for health and disease (Carrico *et al.*
306 2018).

307 Mitochondria of higher eukaryotes typically maintain several copies of their own circular genome
308 known as mitochondrial DNA (mtDNA; hundred to thousands per cell; Cummins 1998), which is
309 maternally inherited in humans. Biparental mitochondrial inheritance is documented in mammals, birds,
310 fish, reptiles and invertebrate groups, and is even the norm in some bivalve taxonomic groups (Breton
311 *et al.* 2007; White *et al.* 2008). The mitochondrial genome of the angiosperm *Amborella* contains a
312 record of six mitochondrial genome equivalents acquired by horizontal transfer of entire genomes, two
313 from angiosperms, three from algae and one from mosses (Rice *et al.* 2016). In unicellular organisms
314 (*i.e.*, protists) the structural organization of mitochondrial genomes is highly variable and includes
315 circular and linear DNA (Zikova *et al.* 2016). While some of the free-living flagellates exhibit the largest
316 known gene coding capacity (*e.g.* jakobid *Andalucia godoyi* mitochondrial DNA codes for 106 genes;
317 Burger *et al.* 2013), some protist groups (*e.g.* alveolates) possess mitochondrial genomes with only three
318 protein-coding genes and two rRNAs (Feagin *et al.* 2012). The complete loss of mitochondrial genome
319 is observed in highly reduced mitochondria of *Cryptosporidium* species (Liu *et al.* 2016). Reaching the
320 final extreme, the microbial eukaryote, oxymonad *Monocercomonoides*, has no mitochondrion
321 whatsoever and lacks all typical nuclear-encoded mitochondrial proteins demonstrating that while in
322 99% of organisms mitochondria play a vital role, this organelle is not indispensable (Karnkowska *et al.*
323 2016).

324 In vertebrates but not all invertebrates, mtDNA is compact (16.5 kB in humans) and encodes 13
325 protein subunits of the transmembrane respiratory Complexes CI, CIII, CIV and ATP synthase (F-
326 ATPase), 22 tRNAs, and two rRNAs. Additional gene content has been suggested to include microRNAs,
327 piRNA, smithRNAs, repeat associated RNA, and even additional proteins (Duarte *et al.* 2014; Lee *et al.*
328 2015; Cobb *et al.* 2016). The mitochondrial genome requires nuclear-encoded mitochondrially
329 targeted proteins, *e.g.*, TFAM, for its maintenance and expression (Rackham *et al.* 2012). Both genomes
330 encode peptides of the membrane spanning redox pumps (CI, CIII and CIV) and F-ATPase, leading to
331 strong constraints in the coevolution of both genomes (Blier *et al.* 2001).

332 Given the multiple roles of mitochondria, it is perhaps not surprising that mitochondrial
333 dysfunction is associated with a wide variety of genetic and degenerative diseases. Robust mitochondrial
334 function is supported by physical exercise and caloric balance, and is central for sustained metabolic
335 health throughout life. Therefore, a more consistent set of definitions for mitochondrial physiology will
336 increase our understanding of the etiology of disease and improve the diagnostic repertoire of
337 mitochondrial medicine with a focus on protective medicine, lifestyle and healthy aging.

338 Mitochondrion is singular and mitochondria is plural. Abbreviation: mt, as generally used in
339 mtDNA.

340

341

342

343 1. Introduction

344

345 Mitochondria are the powerhouses of the cell with numerous physiological, molecular, and
346 genetic functions (**Box 1**). Every study of mitochondrial health and disease faces **Evolution, Age,**
347 **Gender and sex, Lifestyle, and Environment (MitoEAGLE)** as essential background conditions intrinsic
348 to the individual person or cohort, species, tissue and to some extent even cell line. As a large and
349 coordinated group of laboratories and researchers, the mission of the global MitoEAGLE Network is to

350 generate the necessary scale, type, and quality of consistent data sets and conditions to address this
 351 intrinsic complexity. Harmonization of experimental protocols and implementation of a quality control
 352 and data management system are required to interrelate results gathered across a spectrum of studies
 353 and to generate a rigorously monitored database focused on mitochondrial respiratory function. In this
 354 way, researchers from a variety of disciplines can compare their findings using clearly defined and
 355 accepted international standards.

356 With an emphasis on quality of research, published data can be useful far beyond the specific
 357 question of a particular experiment. For example, collaborative data sets support the development of
 358 open-access databases such as those for National Institutes of Health sponsored research in genetics,
 359 proteomics, and metabolomics. Indeed, enabling meta-analytic studies is the most economic way of
 360 providing robust answers to biological questions (Cooper *et al.* 2009). However, the reproducibility of
 361 quantitative results and databases depend on accurate measurements under strictly-defined conditions.
 362 Likewise, meaningful interpretation and comparability of experimental outcomes requires
 363 standardisation of protocols between research groups at different institutes. In addition to quality control,
 364 a conceptual framework is also required to standardise and homogenise terminology and methodology.
 365 Vague or ambiguous jargon can lead to confusion and may relegate valuable signals to wasteful noise.
 366 For this reason, measured values must be expressed in standard units for each parameter used to define
 367 mitochondrial respiratory function. A consensus on fundamental nomenclature and conceptual
 368 coherence, however, are missing in the expanding field of mitochondrial physiology. To fill this gap,
 369 the present communication provides an in-depth review on harmonization of nomenclature and
 370 definition of technical terms, which are essential to improve the awareness of the intricate meaning of
 371 current and past scientific vocabulary. This is important for documentation and integration into
 372 databases in general, and quantitative modelling in particular (Beard 2005).

373 In this review, we focus on coupling states and fluxes through metabolic pathways of aerobic
 374 energy transformation in mitochondrial preparations as a first step in the attempt to generate a
 375 conceptually-oriented nomenclature in bioenergetics and mitochondrial physiology. Respiratory control
 376 by fuel substrates and specific inhibitors of respiratory enzymes, coupling states of intact cells, and
 377 respiratory flux control ratios will be reviewed in subsequent communications, prepared in the frame of
 378 COST Action MitoEAGLE open to global bottom-up input.

379
 380

381 **2. Coupling states and rates in mitochondrial preparations**

382 *‘Every professional group develops its own technical jargon for talking about matters of critical*
 383 *concern ... People who know a word can share that idea with other members of their group, and*
 384 *a shared vocabulary is part of the glue that holds people together and allows them to create a*
 385 *shared culture’* (Miller 1991).

386

387 *2.1. Cellular and mitochondrial respiration*

388

389 **2.1.1. Aerobic and anaerobic catabolism and ATP turnover:** In respiration, electron transfer
 390 is coupled to the phosphorylation of ADP to ATP, with energy transformation mediated by the
 391 protonmotive force, Δp (**Figure 2**). Anabolic reactions are coupled to catabolism, both by ATP as the
 392 intermediary energy currency and by small organic precursor molecules as building blocks for
 393 biosynthesis. Glycolysis involves substrate-level phosphorylation of ADP to ATP in fermentation
 394 without utilization of O₂, studied mainly in intact cells and organisms. Many cellular fuel substrates are
 395 catabolized to acetyl-CoA or to glutamate, and further electron transfer reduces nicotinamide adenine
 396 dinucleotide to NADH or flavin adenine dinucleotide to FADH₂. Subsequent mitochondrial electron
 397 transfer to O₂ is coupled to proton translocation for the control of Δp and phosphorylation of ADP
 398 (**Figure 2B and 2C**). In contrast, extra-mitochondrial oxidation of fatty acids and amino acids proceeds
 399 partially in peroxisomes without coupling to ATP production: acyl-CoA oxidase catalyzes the oxidation
 400 of FADH₂ with electron transfer to O₂; amino acid oxidases oxidize flavin mononucleotide FMNH₂ or
 401 FADH₂ (**Figure 2A**).

402

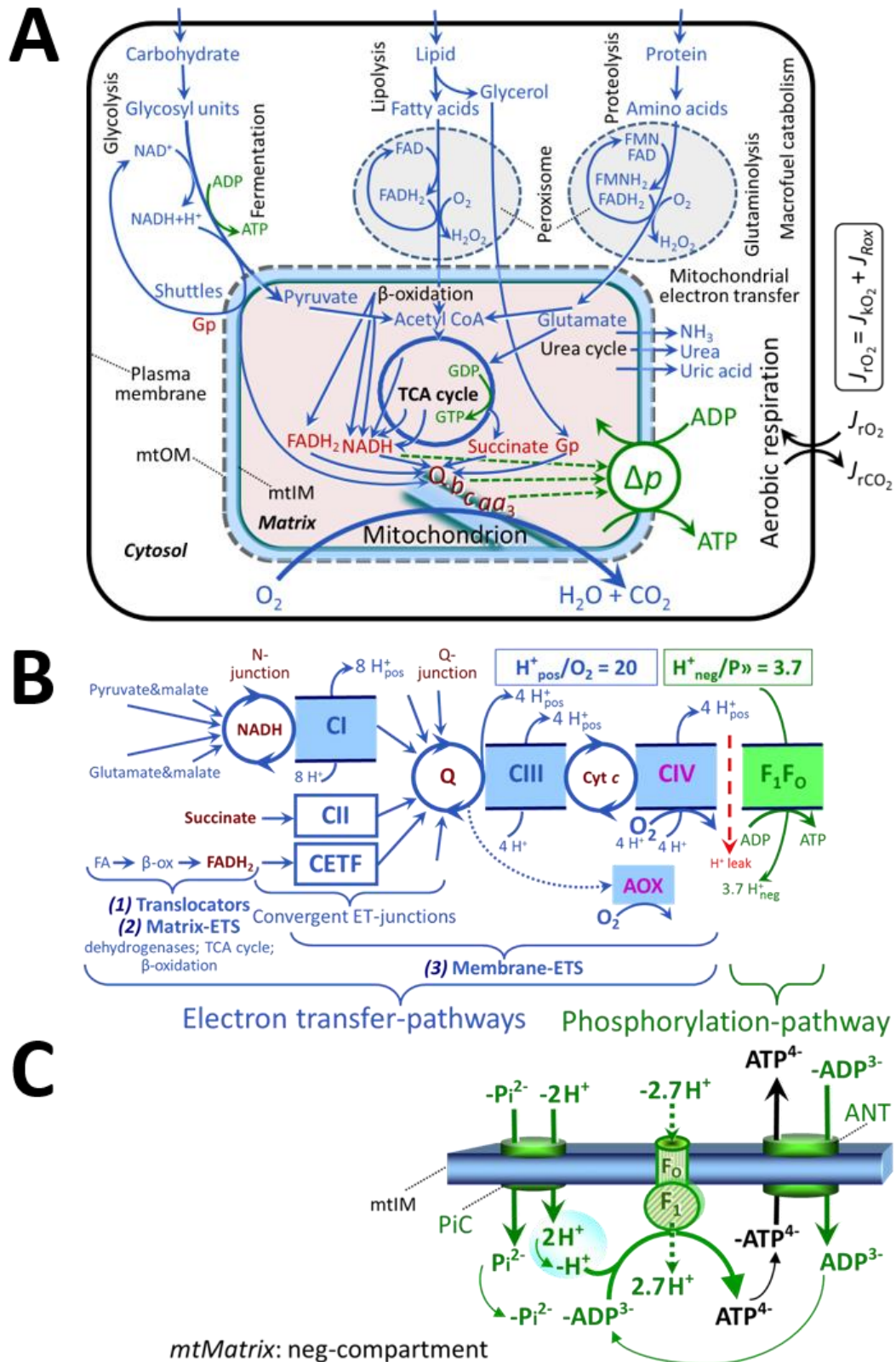


Figure 2. Cell respiration and oxidative phosphorylation (OXPHOS)

Mitochondrial respiration is the oxidation of fuel substrates (electron donors) with electron transfer to O_2 as the electron acceptor. For explanation of symbols see also **Figure 1**.

(A) Respiration of intact cells: Extra-mitochondrial catabolism of macromolecules and uptake of small molecules by the cell provide the mitochondrial fuel substrates. Dashed arrows indicate the connection between the redox proton pumps (respiratory Complexes CI, CIII and CIV) and the transmembrane Δp . Coenzyme Q (Q) and the cytochromes *b*, *c*, and *aa*₃ are redox systems of the mitochondrial inner membrane, mtIM. Glycerol-3-phosphate, Gp.

403
404
405
406
407
408
409
410
411

412 (B) Respiration in mitochondrial preparations: The mitochondrial electron transfer system
 413 (ETS) is (1) fuelled by diffusion and transport of substrates across the mtOM and mtIM,
 414 and in addition consists of the (2) matrix-ETS, and (3) membrane-ETS. Electron transfer
 415 converges at the N-junction, and from CI, CII and electron transferring flavoprotein
 416 complex (CETF) at the Q-junction. Unspecified arrows converging at the Q-junction
 417 indicate additional ETS-sections with electron entry into Q through glycerophosphate
 418 dehydrogenase, dihydro-orotate dehydrogenase, proline dehydrogenase, choline
 419 dehydrogenase, and sulfide-ubiquinone oxidoreductase. The dotted arrow indicates the
 420 branched pathway of oxygen consumption by alternative quinol oxidase (AOX). ET-
 421 pathways are coupled to the phosphorylation-pathway. The H^+_{pos}/O_2 ratio is the outward
 422 proton flux from the matrix space to the positively (pos) charged vesicular compartment,
 423 divided by catabolic O_2 flux in the NADH-pathway. The H^+_{neg}/P_{\gg} ratio is the inward proton
 424 flux from the inter-membrane space to the negatively (neg) charged matrix space, divided
 425 by the flux of phosphorylation of ADP to ATP. These stoichiometries are not fixed due to
 426 ion leaks and proton slip. Modified from (B) Lemieux *et al.* (2017) and Rich (2013).

427 (C) Chemiosmotic phosphorylation-pathway catalyzed by the proton pump F_1F_0 -ATPase
 428 (F-ATPase, ATP synthase), adenine nucleotide translocase (ANT), and inorganic
 429 phosphate carrier (PiC). The H^+_{neg}/P_{\gg} stoichiometry is the sum of the coupling
 430 stoichiometry in the F-ATPase reaction ($-2.7 H^+_{\text{pos}}$ from the positive intermembrane space,
 431 $2.7 H^+_{\text{neg}}$ to the matrix, *i.e.*, the negative compartment) and the proton balance in the
 432 translocation of ADP^{3-} , ATP^{4-} and P_i^{2-} . Modified from Gnaiger (2014).
 433
 434

435 The plasma membrane separates the intracellular compartment including the cytosol, nucleus, and
 436 organelles from the extracellular environment. The plasma membrane consists of a lipid bilayer with
 437 embedded proteins and attached organic molecules that collectively control the selective permeability
 438 of ions, organic molecules, and particles across the cell boundary. The intact plasma membrane prevents
 439 the passage of many water-soluble mitochondrial substrates and inorganic ions—such as succinate,
 440 adenosine diphosphate (ADP) and inorganic phosphate (P_i), that must be precisely controlled at
 441 kinetically-saturating concentrations for the analysis of mitochondrial respiratory capacities.
 442 Respiratory capacities delineate, comparable to channel capacity in information theory (Schneider
 443 2006), the upper bound of the rate of O_2 consumption measured in defined respiratory states. Despite
 444 the activity of solute carriers, *e.g.*, SLC13A3 and SLC20A2, which transport specific metabolites across
 445 the plasma membrane of various cell types, the intact plasma membrane limits the scope of
 446 investigations into mitochondrial respiratory function in intact cells.

447 **2.1.2. Specification of biochemical dose:** Substrates, uncouplers, inhibitors, and other chemical
 448 reagents are titrated to analyse cellular and mitochondrial function. Nominal concentrations of these
 449 substances are usually reported as initial amount of substance concentration [$\text{mol}\cdot\text{L}^{-1}$] in the incubation
 450 medium. When aiming at the measurement of kinetically saturated processes—such as OXPHOS-
 451 capacities, the concentrations for substrates can be chosen according to the apparent equilibrium
 452 constant, K_m' . In the case of hyperbolic kinetics, only 80% of maximum respiratory capacity is obtained
 453 at a substrate concentration of four times the K_m' , whereas substrate concentrations of 5, 9, 19 and 49
 454 times the K_m' are theoretically required for reaching 83%, 90%, 95% or 98% of the maximal rate
 455 (Gnaiger 2001). Other reagents are chosen to inhibit or alter a particular process. The amount of these
 456 chemicals in an experimental incubation is selected to maximize effect, avoiding unacceptable off-target
 457 consequences that would adversely affect the data being sought. Specifying the amount of substance in
 458 an incubation as nominal concentration in the aqueous incubation medium can be ambiguous (Doskey
 459 *et al.* 2015), particularly for cations (TPP^+ ; fluorescent dyes such as safranin, TMRM; Chowdhury *et al.*
 460 2015) and lipophilic substances (oligomycin, uncouplers, permeabilization agents; Doerrier *et al.* 2018),
 461 which accumulate in the mitochondrial matrix or in biological membranes, respectively. Generally,
 462 dose/exposure can be specified per unit of biological sample, *i.e.*, (nominal moles of
 463 xenobiotic)/(number of cells) [$\text{mol}\cdot\text{cell}^{-1}$] or, as appropriate, per mass of biological sample [$\text{mol}\cdot\text{kg}^{-1}$].
 464 This approach to specification of dose/exposure provides a scalable parameter that can be used to design
 465 experiments, help interpret a wide variety of experimental results, and provide absolute information that
 466 allows researchers worldwide to make the most use of published data (Doskey *et al.* 2015).
 467

468 2.2. Mitochondrial preparations

469

470 Mitochondrial preparations are defined as either isolated mitochondria, or tissue and cellular
 471 preparations in which the barrier function of the plasma membrane is disrupted. Since this entails the
 472 loss of cell viability, mitochondrial preparations are not studied *in vivo*. In contrast to isolated
 473 mitochondria and tissue homogenate preparations, mitochondria in permeabilized tissues and cells are
 474 *in situ* relative to the plasma membrane. When studying mitochondrial preparations, substrate-
 475 uncoupler-inhibitor-titration (SUIT) protocols are used to establish respiratory coupling control states
 476 (CCS) and pathway control states (PCS) that provide reference values for various output variables
 477 (**Table 1**). Physiological conditions *in vivo* deviate from these experimentally obtained states; this is
 478 because kinetically-saturating concentrations, *e.g.*, of ADP, oxygen (O₂; dioxygen) or fuel substrates,
 479 may not apply to physiological intracellular conditions. Further information is obtained in studies of
 480 kinetic responses to variations in fuel substrate concentrations, [ADP], or [O₂] in the range between
 481 kinetically-saturating concentrations and anoxia (Gnaiger 2001).

482 The cholesterol content of the plasma membrane is high compared to mitochondrial membranes
 483 (Korn 1969). Therefore, mild detergents—such as digitonin and saponin—can be applied to selectively
 484 permeabilize the plasma membrane via interaction with cholesterol; this allows free exchange of organic
 485 molecules and inorganic ions between the cytosol and the immediate cell environment, while
 486 maintaining the integrity and localization of organelles, cytoskeleton, and the nucleus. Application of
 487 permeabilization agents (mild detergents or toxins) leads to washout of cytosolic marker enzymes—
 488 such as lactate dehydrogenase—and results in the complete loss of cell viability (tested by nuclear
 489 staining using plasma membrane-impermeable dyes), while mitochondrial function remains intact
 490 (tested by cytochrome *c* stimulation of respiration). Digitonin concentrations have to be optimized
 491 according to cell type, particularly since mitochondria from cancer cells contain significantly higher
 492 contents of cholesterol in both membranes (Baggetto and Testa-Perussini, 1990). For example, a dose
 493 of digitonin of 8 fmol·cell⁻¹ (10 pg·cell⁻¹; 10 μg·10⁻⁶ cells) is optimal for permeabilization of endothelial
 494 cells, and the concentration in the incubation medium has to be adjusted according to the cell density
 495 applied (Doerrier *et al.* 2018). Respiration of isolated mitochondria remains unaltered after the addition
 496 of low concentrations of digitonin or saponin. In addition to mechanical cell disruption during
 497 homogenization of tissue, permeabilization agents may be applied to ensure permeabilization of all cells
 498 in tissue homogenates.

499 Suspensions of cells permeabilized in the respiration chamber and crude tissue homogenates
 500 contain all components of the cell at highly dilute concentrations. All mitochondria are retained in
 501 chemically-permeabilized mitochondrial preparations and crude tissue homogenates. In the preparation
 502 of isolated mitochondria, however, the mitochondria are separated from other cell fractions and purified
 503 by differential centrifugation, entailing the loss of mitochondria at typical recoveries ranging from 30%
 504 to 80% of total mitochondrial content (Lai *et al.* 2018). Using Percoll or sucrose density gradients to
 505 maximize the purity of isolated mitochondria may compromise the mitochondrial yield or structural and
 506 functional integrity. Therefore, mitochondrial isolation protocols need to be optimized according to each
 507 study. The term mitochondrial preparation does neither include intact cells, nor submitochondrial
 508 particles and further fractionation of mitochondrial components.

509

510 2.3. Electron transfer pathways

511

512 Mitochondrial electron transfer (ET) pathways are fuelled by diffusion and transport of substrates
 513 across the mtOM and mtIM. In addition, the mitochondrial electron transfer system (ETS) consists of
 514 the matrix-ETS, and membrane-ETS (**Figure 2B**). Upstream sections of ET-pathways converge at the
 515 NADH-junction (N-junction). NADH is mainly generated in the tricarboxylic acid (TCA) cycle and is
 516 oxidized by Complex I (CI), with further electron entry into the coenzyme Q-junction (Q-junction).
 517 Similarly, succinate is formed in the TCA cycle and oxidized by CII to fumarate. CII is part of both the
 518 TCA cycle and the ETS, and reduces FAD to FADH₂ with further reduction of ubiquinone to ubiquinol
 519 downstream of the TCA cycle in the Q-junction. Thus FADH₂ is not a substrate but is the product of
 520 CII, in contrast to erroneous metabolic maps shown in many publications. β-oxidation of fatty acids
 521 (FA) generates FADH₂ as the substrate of electron transferring flavoprotein complex (ETF).

522 Selected mitochondrial catabolic pathways, *k*, of electron transfer from the oxidation of fuel
 523 substrates to the reduction of O₂ are activated by depletion of endogenous substrates and addition of fuel

524 substrates to the mitochondrial respiration medium (**Figure 2B**). Substrate combinations and specific
 525 inhibitors of ET-pathway enzymes are used to obtain defined pathway control states in mitochondrial
 526 preparations (Gnaiger 2014).

527

528 2.4. Respiratory coupling control

529

530 **2.4.1. Coupling:** In mitochondrial electron transfer, vectorial transmembrane proton flux is
 531 coupled through the redox proton pumps CI, CIII and CIV to the catabolic flux of scalar reactions,
 532 collectively measured as O₂ flux, J_{KO_2} (**Figure 2**). Thus mitochondria are elementary components of
 533 energy transformation. Energy is a conserved quantity and cannot be lost or produced in any internal
 534 process (First Law of thermodynamics). Open and closed systems can gain or lose energy only by
 535 external fluxes—by exchange with the environment. Therefore, energy can neither be produced by
 536 mitochondria, nor is there any internal process without energy conservation. Exergy or Gibbs energy
 537 (‘free energy’) is the part of energy that can potentially be transformed into work under conditions of
 538 constant temperature and pressure. *Coupling* is the interaction of an exergonic process (spontaneous,
 539 negative exergy change) with an endergonic process (positive exergy change) in energy transformations
 540 which conserve part of the exergy that would be irreversibly lost or dissipated in an uncoupled process.

541 Pathway control states (PCS) and coupling control states (CCS) are complementary, since
 542 mitochondrial preparations depend on (1) an exogenous supply of pathway-specific fuel substrates and
 543 oxygen, and (2) exogenous control of phosphorylation (**Figure 2**).

544 **2.4.2. Phosphorylation, P», and P»/O₂ ratio:** Phosphorylation in the context of OXPHOS is
 545 defined as phosphorylation of ADP by P_i to form ATP. On the other hand, the term phosphorylation is
 546 used generally in many contexts, *e.g.*, protein phosphorylation. This justifies consideration of a symbol
 547 more discriminating and specific than P as used in the P/O ratio (phosphate to atomic oxygen ratio),
 548 where P indicates phosphorylation of ADP to ATP or GDP to GTP (**Figure 2**). We propose the symbol
 549 P» for the endergonic (uphill) direction of phosphorylation ADP→ATP, and likewise the symbol P« for
 550 the corresponding exergonic (downhill) hydrolysis ATP→ADP. P» refers mainly to electrontransfer
 551 phosphorylation but may also involve substrate-level phosphorylation as part of the TCA cycle
 552 (succinyl-CoA ligase; phosphoglycerate kinase) and phosphorylation of ADP catalyzed by pyruvate
 553 kinase, and of GDP phosphorylated by phosphoenolpyruvate carboxykinase. Transphosphorylation is
 554 performed by adenylate kinase, creatine kinase (mtCK), hexokinase and nucleoside diphosphate kinase.
 555 In isolated mammalian mitochondria, ATP production catalyzed by adenylate kinase (2 ADP ↔ ATP +
 556 AMP) proceeds without fuel substrates in the presence of ADP (Komlódi and Tretter 2017). Kinase
 557 cycles are involved in intracellular energy transfer and signal transduction for regulation of energy flux.

558 The P»/O₂ ratio (P»/4 e⁻) is two times the ‘P/O’ ratio (P»/2 e⁻) of classical bioenergetics. P»/O₂ is
 559 a generalized symbol, not specific for determination of P_i consumption (P_i/O₂ flux ratio), ADP depletion
 560 (ADP/O₂ flux ratio), or ATP production (ATP/O₂ flux ratio). The mechanistic P»/O₂ ratio—or P»/O₂
 561 stoichiometry—is calculated from the proton-to-O₂ and proton-to-phosphorylation coupling
 562 stoichiometries (**Figure 2B**):

563

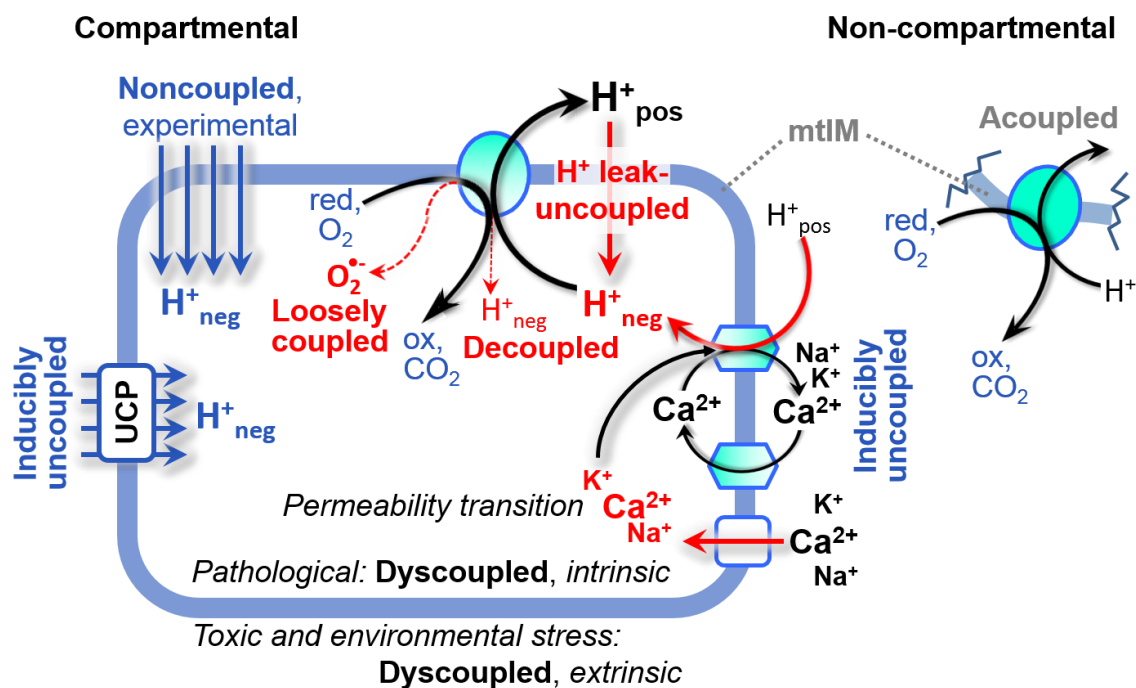
$$564 \quad P»/O_2 = \frac{H_{\text{pos}}^+/O_2}{H_{\text{neg}}^+/P»} \quad (1)$$

565

566 The H⁺_{pos}/O₂ coupling stoichiometry (referring to the full 4 electron reduction of O₂) depends on the
 567 relative involvement of the three coupling sites (respiratory Complexes CI, CIII and CIV) in the
 568 catabolic ET-pathway from reduced fuel substrates (electron donors) to the reduction of O₂ (electron
 569 acceptor). This varies with: (1) a bypass of CI by single or multiple electron input into the Q-junction;
 570 and (2) a bypass of CIV by involvement of alternative oxidases, AOX, which are not expressed in
 571 mammalian mitochondria.

572 The H⁺_{pos}/O₂ coupling stoichiometry equals 12 in the ET-pathways involving CIII and CIV as
 573 proton pumps, increasing to 20 for the NADH-pathway through CI (**Figure 2B**), but a general consensus
 574 on H⁺_{pos}/O₂ stoichiometries remains to be reached (Hinkle 2005; Wikström and Hummer 2012; Sazanov
 575 2015). The H⁺_{neg}/P» coupling stoichiometry (3.7; **Figure 2B**) is the sum of 2.7 H⁺_{neg} required by the F-
 576 ATPase of vertebrate and most invertebrate species (Watt *et al.* 2010) and the proton balance in the
 577 translocation of ADP, ATP and P_i (**Figure 2C**). Taken together, the mechanistic P»/O₂ ratio is calculated
 578 at 5.4 and 3.3 for NADH- and succinate-linked respiration, respectively (Eq. 1). The corresponding

579 classical P_»/O ratios (referring to the 2 electron reduction of 0.5 O₂) are 2.7 and 1.6 (Watt *et al.* 2010),
 580 in agreement with the measured P_»/O ratio for succinate of 1.58 ± 0.02 (Gnaiger *et al.* 2000).
 581



582
 583 **Figure 3. Mechanisms of respiratory uncoupling**
 584 An intact mitochondrial inner membrane, mtIM, is required for vectorial, compartmental coupling.
 585 'Acoupled' respiration is the consequence of structural disruption with catalytic activity of non-
 586 compartmental mitochondrial fragments. Inducible uncoupling (*e.g.*, by activation of UCP1) increases
 587 LEAK respiration; experimentally noncoupled respiration provides an estimate of ET-capacity obtained
 588 by titration of protonophores stimulating respiration to maximum O₂ flux. H⁺ leak-uncoupled,
 589 decoupled, and loosely coupled respiration are components of intrinsic uncoupling (**Table 2**).
 590 Pathological dysfunction may affect all types of uncoupling, including permeability transition, causing
 591 intrinsically dyscoupled respiration. Similarly, toxicological and environmental stress factors can cause
 592 extrinsically dyscoupled respiration. Reduced fuel substrates, red; oxidized products, ox.
 593

594 **2.4.3. Uncoupling:** The effective P_»/O₂ flux ratio ($Y_{P_{»}/O_2} = J_{P_{»}}/J_{K_{O_2}}$) is diminished relative to the
 595 mechanistic P_»/O₂ ratio by intrinsic and extrinsic uncoupling or dyscoupling (**Figure 3**). Such
 596 generalized uncoupling is different from switching to mitochondrial pathways that involve fewer than
 597 three proton pumps ('coupling sites': Complexes CI, CIII and CIV), bypassing CI through multiple
 598 electron entries into the Q-junction, or CIII and CIV through AOX (**Figure 2B**). Reprogramming of
 599 mitochondrial pathways leading to different types of substrates being oxidized may be considered as a
 600 switch of gears (changing the stoichiometry by altering the substrate that is oxidized) rather than
 601 uncoupling (loosening the tightness of coupling relative to a fixed stoichiometry). In addition, $Y_{P_{»}/O_2}$
 602 depends on several experimental conditions of flux control, increasing as a hyperbolic function of [ADP]
 603 to a maximum value (Gnaiger 2001).

604 Uncoupling of mitochondrial respiration is a general term comprising diverse mechanisms:

- 605 1. Proton leak across the mtIM from the pos- to the neg-compartment (H⁺ leak-uncoupled; **Figure**
 606 **3**).
- 607 2. Cycling of other cations, strongly stimulated by permeability transition; comparable to the use of
 608 protonophores, cation cycling is experimentally induced by valinomycin in the presence of K⁺;
- 609 3. Decoupling by proton slip in the redox proton pumps when protons are effectively not pumped
 610 (CI, CIII and CIV) or are not driving phosphorylation (F-ATPase);
- 611 4. Loss of vesicular (compartmental) integrity when electron transfer is acoupled;
- 612 5. Electron leak in the loosely coupled univalent reduction of O₂ to superoxide (O₂⁻; superoxide
 613 anion radical).

614 Differences of terms—uncoupled *vs.* noncoupled—are easily overlooked, although they relate to
 615 different meanings of uncoupling (**Figure 3** and **Table 2**).

616

617 2.5. Coupling states and respiratory rates

618

619 To extend the classical nomenclature on mitochondrial coupling states (Section 2.6) by a concept-
 620 driven terminology that explicitly incorporates information on the meaning of respiratory states, the
 621 terminology must be general and not restricted to any particular experimental protocol or mitochondrial
 622 preparation (Gnaiger 2009). Concept-driven nomenclature aims at mapping the meaning and concept
 623 behind the words and acronyms onto the forms of words and acronyms (Miller 1991). The focus of
 624 concept-driven nomenclature is primarily the conceptual *why*, along with clarification of the
 625 experimental *how*.

626

627 **Table 1. Coupling states and residual oxygen consumption in mitochondrial**
 628 **preparations in relation to respiration- and phosphorylation-flux, J_{KO_2} and J_{P_\ast} , and**
 629 **protonmotive force, Δp .** Coupling states are established at kinetically-saturating
 630 concentrations of fuel substrates and O_2 .

| State | J_{KO_2} | J_{P_\ast} | Δp | Inducing factors | Limiting factors |
|--------|--|---------------------|------------|--|---|
| LEAK | <i>L</i> ; low, cation leak-dependent respiration | 0 | max. | back-flux of cations including proton leak, proton slip | $J_{\text{P}_\ast} = 0$: (1) without ADP, L_{N} ; (2) max. ATP/ADP ratio, L_{T} ; or (3) inhibition of the phosphorylation-pathway, L_{Omy} |
| OXPHOS | <i>P</i> ; high, ADP-stimulated respiration, OXPHOS-capacity | max. | high | kinetically-saturating [ADP] and [P_i] | J_{P_\ast} by phosphorylation-pathway; or J_{KO_2} by ET-capacity |
| ET | <i>E</i> ; max., noncoupled respiration, ET-capacity | 0 | low | optimal external uncoupler concentration for max. $J_{\text{O}_2, \text{E}}$ | J_{KO_2} by ET-capacity |
| ROX | <i>Rox</i> ; min., residual O_2 consumption | 0 | 0 | $J_{\text{O}_2, \text{Rox}}$ in non-ET-pathway oxidation reactions | inhibition of all ET-pathways; or absence of fuel substrates |

631

632 To provide a diagnostic reference for respiratory capacities of core energy metabolism, the
 633 capacity of oxidative phosphorylation, OXPHOS, is measured at kinetically-saturating concentrations
 634 of ADP and P_i . The oxidative ET-capacity reveals the limitation of OXPHOS-capacity mediated by the
 635 phosphorylation-pathway. The ET- and phosphorylation-pathways comprise coupled segments of the
 636 OXPHOS-system. ET-capacity is measured as noncoupled respiration by application of external
 637 uncouplers. The contribution of intrinsically uncoupled O_2 consumption is studied by preventing the
 638 stimulation of phosphorylation either in the absence of ADP or by inhibition of the phosphorylation-
 639 pathway. The corresponding states are collectively classified as LEAK-states, when O_2 consumption
 640 compensates mainly for ion leaks, including the proton leak. Defined coupling states are induced by: (1)
 641 adding cation chelators such as EGTA, binding free Ca^{2+} and thus limiting cation cycling; (2) adding
 642 ADP and P_i ; (3) inhibiting the phosphorylation-pathway; and (4) uncoupler titrations, while maintaining
 643 a defined ET-pathway state with constant fuel substrates and inhibitors of specific branches of the ET-
 644 pathway.

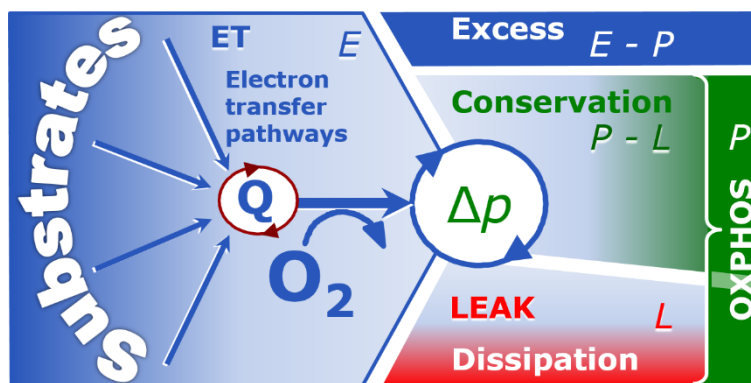
645

646 The three coupling states, ET, LEAK and OXPHOS, are shown schematically with the
 647 corresponding respiratory rates, abbreviated as *E*, *L* and *P*, respectively (**Figure 4**). We distinguish
 648 metabolic *pathways* from metabolic *states* and the corresponding metabolic *rates*; for example: ET-
 649 pathways, ET-states, and ET-capacities, *E*, respectively (**Table 1**). The protonmotive force is *high* in
 the OXPHOS-state when it drives phosphorylation, *maximum* in the LEAK-state of coupled

650 mitochondria, driven by LEAK-respiration at a minimum back-flux of cations to the matrix side, and
 651 *very low* in the ET-state when uncouplers short-circuit the proton cycle (Table 1).
 652

653 **Figure 4. Four-compartment**
 654 **model of oxidative**
 655 **phosphorylation**

656 Respiratory states (ET, OXPHOS, LEAK; Table 1) and corresponding
 657 rates (E , P , L) are connected by the
 658 protonmotive force, Δp . (1) ET-
 659 capacity, E , is partitioned into (2)
 660 dissipative LEAK-respiration, L ,
 661 when the Gibbs energy change of
 662 catabolic O_2 flux is irreversibly lost,
 663 (3) net OXPHOS-capacity, $P-L$, with
 664 partial conservation of the capacity to perform work, and (4) the excess capacity, $E-P$. Modified from
 665 Gnaiger (2014).
 666



667 **Figure 5. Respiratory coupling**
 668 **states**

669 **(A) LEAK-state and rate, L :**

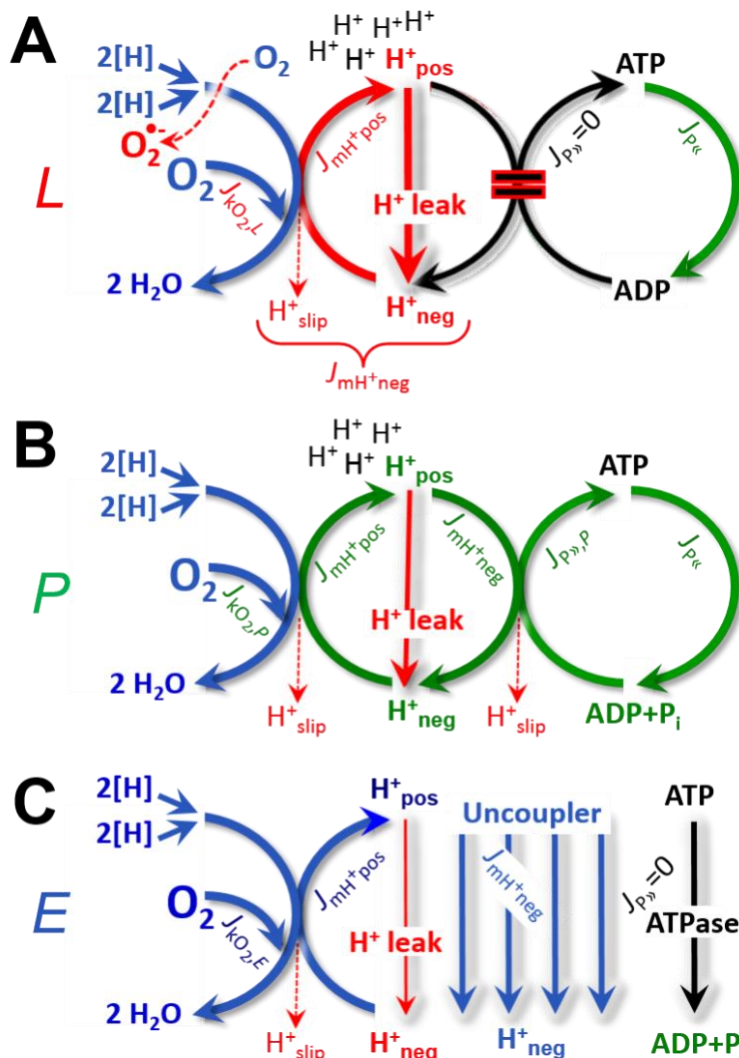
670 Oxidation only, since
 671 phosphorylation is arrested, $J_{P\gg} = 0$,
 672 and catabolic O_2 flux, $J_{kO_2,L}$,
 673 is controlled mainly by the proton leak
 674 and slip, J_{mH^+neg} , at maximum
 675 protonmotive force (Figure 4).
 676 Extramitochondrial ATP may be
 677 hydrolyzed by extramitochondrial
 678 ATPases, $J_{P\ll}$.

679 **(B) OXPHOS-state and rate, P :**

680 Oxidation coupled
 681 to phosphorylation, $J_{P\gg}$, which is
 682 stimulated by kinetically-saturating
 683 [ADP] and $[P_i]$, supported by a high
 684 protonmotive force. O_2 flux, $J_{kO_2,P}$,
 685 is well-coupled at a $P\gg/O_2$ ratio of
 686 $J_{P\gg,P}/J_{O_2,P}$. Extramitochondrial
 687 ATPases may recycle ATP, $J_{P\ll}$.

688 **(C) ET-state and rate, E :**

689 Oxidation only, since phosphorylation is zero,
 690 $J_{P\gg} = 0$, at optimum exogenous
 691 uncoupler concentration when
 692 noncoupled respiration, $J_{kO_2,E}$, is
 693 maximum. The F-ATPase may
 694 hydrolyze extramitochondrial ATP.



667
 668 **2.5.1. LEAK-state (Figure 5A):** The LEAK-state is defined as a state of mitochondrial
 669 respiration when O_2 flux mainly compensates for ion leaks in the absence of ATP synthesis, at
 670 kinetically-saturating concentrations of O_2 , respiratory fuel substrates and P_i . LEAK-respiration is
 671 measured to obtain an estimate of intrinsic uncoupling without addition of an experimental uncoupler:
 672 (1) in the absence of adenylates, *i.e.*, AMP, ADP and ATP; (2) after depletion of ADP at a maximum
 673 ATP/ADP ratio; or (3) after inhibition of the phosphorylation-pathway by inhibitors of F-ATPase—such

674 as oligomycin, or of adenine nucleotide translocase—such as carboxyatractyloside. Adjustment of the
 675 nominal concentration of these inhibitors to the density of biological sample applied can minimize or
 676 avoid inhibitory side-effects exerted on ET-capacity or even some dyscoupling.

- 677 • **Proton leak and uncoupled respiration:** The intrinsic proton leak is the *uncoupled* leak current
 678 of protons in which protons diffuse across the mtIM in the dissipative direction of the downhill
 679 protonmotive force without coupling to phosphorylation (**Figure 5A**). The proton leak flux
 680 depends non-linearly on the protonmotive force (Garlid *et al.* 1989; Divakaruni and Brand 2011),
 681 which is a temperature-dependent property of the mtIM and may be enhanced due to possible
 682 contaminations by free fatty acids. Inducible uncoupling mediated by uncoupling protein 1
 683 (UCP1) is physiologically controlled, *e.g.*, in brown adipose tissue. UCP1 is a member of the
 684 mitochondrial carrier family that is involved in the translocation of protons across the mtIM
 685 (Klingenberg 2017). Consequently, this short-circuit lowers the protonmotive force and
 686 stimulates electron transfer, respiration, and heat dissipation in the absence of phosphorylation of
 687 ADP.
- 688 • **Cation cycling:** There can be other cation contributors to leak current including calcium and
 689 probably magnesium. Calcium influx is balanced by mitochondrial $\text{Na}^+/\text{Ca}^{2+}$ or $\text{H}^+/\text{Ca}^{2+}$
 690 exchange, which is balanced by Na^+/H^+ or K^+/H^+ exchanges. This is another effective uncoupling
 691 mechanism different from proton leak (**Table 2**).
 692
 693

Table 2. Terms on respiratory coupling and uncoupling.

| Term | J_{kO_2} | $\text{P}\gg/\text{O}_2$ | Notes | |
|----------------------------------|-----------------------|--------------------------|---|---|
| acoupled | | 0 | electron transfer in mitochondrial fragments without vectorial proton translocation (Figure 3) | |
| intrinsic, no protonophore added | uncoupled | L | 0 | non-phosphorylating LEAK-respiration (Figure 5A) |
| | proton leak-uncoupled | | 0 | component of L , H^+ diffusion across the mtIM (Figure 3) |
| | decoupled | | 0 | component of L , proton slip (Figure 3) |
| | loosely coupled | | 0 | component of L , lower coupling due to superoxide formation and bypass of proton pumps by electron leak (Figure 3) |
| | dyscoupled | | 0 | pathologically, toxicologically, environmentally increased uncoupling, mitochondrial dysfunction |
| | inducibly uncoupled | | 0 | by UCP1 or cation (<i>e.g.</i> , Ca^{2+}) cycling (Figure 3) |
| noncoupled | E | 0 | ET-capacity, non-phosphorylating respiration stimulated to maximum flux at optimum exogenous uncoupler concentration (Figure 5C) | |
| well-coupled | P | high | OXPHOS-capacity , phosphorylating respiration with an intrinsic LEAK component (Figure 5B) | |
| fully coupled | $P - L$ | max. | OXPHOS-capacity corrected for LEAK-respiration (Figure 4) | |

- 694 • **Proton slip and decoupled respiration:** Proton slip is the *decoupled* process in which protons
 695 are only partially translocated by a redox proton pump of the ET-pathways and slip back to the
 696 original vesicular compartment. The proton leak is the dominant contributor to the overall leak
 697 current in mammalian mitochondria incubated under physiological conditions at 37 °C, whereas
 698 proton slip increases at lower experimental temperature (Canton *et al.* 1995). Proton slip can also
 699 happen in association with the F-ATPase, in which the proton slips downhill across the pump to
 700 the matrix without contributing to ATP synthesis. In each case, proton slip is a property of the
 701 proton pump and increases with the pump turnover rate.
 702

- 703 • **Electron leak and loosely coupled respiration:** Superoxide production by the ETS leads to a
704 bypass of redox proton pumps and correspondingly lower P_{\gg}/O_2 ratio. This depends on the actual
705 site of electron leak and the scavenging of hydrogen peroxide by cytochrome *c*, whereby electrons
706 may re-enter the ETS with proton translocation by CIV.
- 707 • **Loss of compartmental integrity and acoupled respiration:** Electron transfer and catabolic O_2
708 flux proceed without compartmental proton translocation in disrupted mitochondrial fragments.
709 Such fragments are an artefact of mitochondrial isolation, and may not fully fuse to re-establish
710 structurally intact mitochondria. Loss of mtIM integrity, therefore, is the cause of acoupled
711 respiration, which is a nonvectorial dissipative process without control by the protonmotive force.
- 712 • **Dyscoupled respiration:** Mitochondrial injuries may lead to *dyscoupling* as a pathological or
713 toxicological cause of *uncoupled* respiration. Dyscoupling may involve any type of uncoupling
714 mechanism, *e.g.*, opening the permeability transition pore. Dyscoupled respiration is
715 distinguished from the experimentally induced *noncoupled* respiration in the ET-state (**Table 2**).
716

717 **2.5.2. OXPHOS-state (Figure 5B):** The OXPHOS-state is defined as the respiratory state with
718 kinetically-saturating concentrations of O_2 , respiratory and phosphorylation substrates, and absence of
719 exogenous uncoupler, which provides an estimate of the maximal respiratory capacity in the OXPHOS-
720 state for any given ET-pathway state. Respiratory capacities at kinetically-saturating substrate
721 concentrations provide reference values or upper limits of performance, aiming at the generation of data
722 sets for comparative purposes. Physiological activities and effects of substrate kinetics can be evaluated
723 relative to the OXPHOS-capacity.

724 As discussed previously, 0.2 mM ADP does not fully saturate flux in isolated mitochondria
725 (Gnaiger 2001; Puchowicz *et al.* 2004); greater [ADP] is required, particularly in permeabilized muscle
726 fibres and cardiomyocytes, to overcome limitations by intracellular diffusion and by the reduced
727 conductance of the mtOM (Jepihhina *et al.* 2011, Illaste *et al.* 2012, Simson *et al.* 2016), either through
728 interaction with tubulin (Rostovtseva *et al.* 2008) or other intracellular structures (Birkedal *et al.* 2014).
729 In addition, saturating ADP concentrations need to be evaluated under different experimental conditions
730 such as temperature (Lemieux *et al.* 2017) and with different animal models (Blier and Guderley, 1993).
731 In permeabilized muscle fibre bundles of high respiratory capacity, the apparent K_m for ADP increases
732 up to 0.5 mM (Saks *et al.* 1998), consistent with experimental evidence that >90% saturation is reached
733 only at >5 mM ADP (Pesta and Gnaiger 2012). Similar ADP concentrations are also required for
734 accurate determination of OXPHOS-capacity in human clinical cancer samples and permeabilized cells
735 (Klepinin *et al.* 2016; Koit *et al.* 2017). Whereas 2.5 to 5 mM ADP is sufficient to obtain the actual
736 OXPHOS-capacity in many types of permeabilized tissue and cell preparations, experimental validation
737 is required in each specific case.

738 **2.5.3. Electron transfer-state (Figure 5C):** O_2 flux determined in the ET-state yields an estimate
739 of ET-capacity. The ET-state is defined as the *noncoupled* state with kinetically-saturating
740 concentrations of O_2 , respiratory substrate and optimum exogenous uncoupler concentration for
741 maximum O_2 flux. Uncouplers are weak lipid-soluble acids which function as protonophores. These
742 disrupt the barrier function of the mtIM and thus short circuit the protonmotive system, functioning like
743 a clutch in a mechanical system. As a consequence of the nearly collapsed protonmotive force, the
744 driving force is insufficient for phosphorylation, and $J_{P_{\gg}} = 0$. The most frequently used uncouplers are
745 carbonyl cyanide *m*-chloro phenyl hydrazone (CCCP), carbonyl cyanide *p*-
746 trifluoromethoxyphenylhydrazone (FCCP), or dinitrophenole (DNP). Stepwise titration of uncouplers
747 stimulates respiration up to or above the level of O_2 consumption rates in the OXPHOS-state; respiration
748 is inhibited, however, above optimum uncoupler concentrations (Mitchell 2011). Data obtained with a
749 single dose of uncoupler must be evaluated with caution, particularly when a fixed uncoupler
750 concentration is used in studies exploring a treatment or disease that may alter the mitochondrial content
751 or mitochondrial sensitivity to inhibition by uncouplers. The effect on ET-capacity of the reversed
752 function of F-ATPase ($J_{P_{\ll}}$; **Figure 5C**) can be evaluated in the presence and absence of
753 extramitochondrial ATP.

754 **2.5.4. ROX state and *Rox*:** Besides the three fundamental coupling states of mitochondrial
755 preparations, the state of residual O_2 consumption, ROX, is relevant to assess respiratory function
756 (**Figure 1**). ROX is not a coupling state. The rate of residual oxygen consumption, *Rox*, is defined as O_2
757 consumption due to oxidative reactions measured after inhibition of ET—with rotenone, malonic acid
758 and antimycin A. Cyanide and azide inhibit not only CIV but catalase and several peroxidases involved

759 in *Rox*. High concentrations of antimycin A, but not rotenone or cyanide, inhibit peroxisomal acyl-CoA
 760 oxidase and D-amino acid oxidase (Vamecq *et al.* 1987). *Rox* represents a baseline that is used to correct
 761 respiration measured in defined coupling states. *Rox*-corrected *L*, *P* and *E* not only lower the values of
 762 total fluxes, but also change the flux control ratios *L/P* and *L/E*. *Rox* is not necessarily equivalent to non-
 763 mitochondrial reduction of O₂, considering O₂-consuming reactions in mitochondria that are not related
 764 to ET—such as O₂ consumption in reactions catalyzed by monoamine oxidases (type A and B),
 765 monooxygenases (cytochrome P450 monooxygenases), dioxygenase (sulfur dioxygenase and
 766 trimethyllysine dioxygenase), and several hydroxylases. Even isolated mitochondrial fractions,
 767 especially those obtained from liver, may be contaminated by peroxisomes. This fact makes the exact
 768 determination of mitochondrial O₂ consumption and mitochondria-associated generation of reactive
 769 oxygen species complicated (Schönfeld *et al.* 2009; Speijer 2016; **Figure 2**). The dependence of ROX-
 770 linked O₂ consumption needs to be studied in detail together with non-ET enzyme activities, availability
 771 of specific substrates, O₂ concentration, and electron leakage leading to the formation of reactive oxygen
 772 species.

773 **2.5.5. Quantitative relations:** *E* may exceed or be equal to *P*. $E > P$ is observed in many types
 774 of mitochondria, varying between species, tissues and cell types (Gnaiger 2009). *E-P* is the excess ET-
 775 capacity pushing the phosphorylation-flux (**Figure 2C**) to the limit of its capacity of utilizing the
 776 protonmotive force. In addition, the magnitude of *E-P* depends on the tightness of respiratory coupling
 777 or degree of uncoupling, since an increase of *L* causes *P* to increase towards the limit of *E*. The *excess*
 778 *E-P* capacity, *E-P*, therefore, provides a sensitive diagnostic indicator of specific injuries of the
 779 phosphorylation-pathway, under conditions when *E* remains constant but *P* declines relative to controls
 780 (**Figure 4**). Substrate cocktails supporting simultaneous convergent electron transfer to the Q-junction
 781 for reconstitution of TCA cycle function establish pathway control states with high ET-capacity, and
 782 consequently increase the sensitivity of the *E-P* assay.

783 *E* cannot theoretically be lower than *P*. $E < P$ must be discounted as an artefact, which may be
 784 caused experimentally by: (1) loss of oxidative capacity during the time course of the respirometric
 785 assay, since *E* is measured subsequently to *P*; (2) using insufficient uncoupler concentrations; (3) using
 786 high uncoupler concentrations which inhibit ET (Gnaiger 2008); (4) high oligomycin concentrations
 787 applied for measurement of *L* before titrations of uncoupler, when oligomycin exerts an inhibitory effect
 788 on *E*. On the other hand, the excess ET-capacity is overestimated if non-saturating [ADP] or [P_i] are
 789 used. See State 3 in the next section.

790 The net OXPHOS-capacity is calculated by subtracting *L* from *P* (**Figure 4**). The net P_»/O₂ equals
 791 P_»/(*P-L*), wherein the dissipative LEAK component in the OXPHOS-state may be overestimated. This
 792 can be avoided by measuring LEAK-respiration in a state when the protonmotive force is adjusted to its
 793 slightly lower value in the OXPHOS-state—by titration of an ET inhibitor (Divakaruni and Brand 2011).
 794 Any turnover-dependent components of proton leak and slip, however, are underestimated under these
 795 conditions (Garlid *et al.* 1993). In general, it is inappropriate to use the term *ATP production* or *ATP*
 796 *turnover* for the difference of O₂ flux measured in the OXPHOS and LEAK states. *P-L* is the upper limit
 797 of OXPHOS-capacity that is freely available for ATP production (corrected for LEAK-respiration) and
 798 is fully coupled to phosphorylation with a maximum mechanistic stoichiometry (**Figure 4**).

799 The rates of LEAK respiration and OXPHOS capacity depend on (1) the tightness of coupling
 800 under the influence of the respiratory uncoupling mechanisms (**Figure 3**), and (2) the coupling
 801 stoichiometry, which varies as a function of the substrate type undergoing oxidation in ET-pathways
 802 with either two or three coupling sites (**Figure 2B**). When cocktails with NADH-linked substrates and
 803 succinate are used, the relative contribution of ET-pathways with three or two coupling sites cannot be
 804 controlled experimentally, is difficult to determine, and may shift in transitions between LEAK-,
 805 OXPHOS- and ET-states (Gnaiger 2014). Under these experimental conditions, we cannot separate the
 806 tightness of coupling *versus* coupling stoichiometry as the mechanisms of respiratory control in the shift
 807 of *L/P* ratios. The tightness of coupling and fully coupled O₂ flux, *P-L* (**Table 2**), therefore, are obtained
 808 from measurements of coupling control of LEAK respiration, OXPHOS- and ET-capacities in well
 809 defined pathway states, using either pyruvate and malate as substrates or the classical succinate and
 810 rotenone substrate-inhibitor combination (**Figure 2B**).

811 **2.5.6. The steady-state:** Mitochondria represent a thermodynamically open system in non-
 812 equilibrium states of biochemical energy transformation. State variables (protonmotive force; redox
 813 states) and metabolic *rates* (fluxes) are measured in defined mitochondrial respiratory *states*. Steady-
 814 states can be obtained only in open systems, in which changes by internal transformations, *e.g.*, O₂

815 consumption, are instantaneously compensated for by external fluxes, *e.g.*, O₂ supply, preventing a
 816 change of O₂ concentration in the system (Gnaiger 1993b). Mitochondrial respiratory states monitored
 817 in closed systems satisfy the criteria of pseudo-steady states for limited periods of time, when changes
 818 in the system (concentrations of O₂, fuel substrates, ADP, P_i, H⁺) do not exert significant effects on
 819 metabolic fluxes (respiration, phosphorylation). Such pseudo-steady states require respiratory media
 820 with sufficient buffering capacity and substrates maintained at kinetically-saturating concentrations, and
 821 thus depend on the kinetics of the processes under investigation.

822

823 2.6. Classical terminology for isolated mitochondria

824 *'When a code is familiar enough, it ceases appearing like a code; one forgets that there is a*
 825 *decoding mechanism. The message is identical with its meaning'* (Hofstadter 1979).

826

827 Chance and Williams (1955; 1956) introduced five classical states of mitochondrial respiration
 828 and cytochrome redox states. **Table 3** shows a protocol with isolated mitochondria in a closed
 829 respirometric chamber, defining a sequence of respiratory states. States and rates are not specifically
 830 distinguished in this nomenclature.

831

832

Table 3. Metabolic states of mitochondria (Chance and Williams, 1956; Table V).

833

834

| State | [O ₂] | ADP level | Substrate level | Respiration rate | Rate-limiting substance |
|-------|-------------------|-----------|-----------------|------------------|-------------------------|
| 1 | >0 | low | low | slow | ADP |
| 2 | >0 | high | ~0 | slow | substrate |
| 3 | >0 | high | high | fast | respiratory chain |
| 4 | >0 | low | high | slow | ADP |
| 5 | 0 | high | high | 0 | oxygen |

835

836 **2.6.1. State 1** is obtained after addition of isolated mitochondria to air-saturated
 837 isoosmotic/isotonic respiration medium containing P_i, but no fuel substrates and no adenylates, *i.e.*,
 838 AMP, ADP, ATP.

839 **2.6.2. State 2** is induced by addition of a 'high' concentration of ADP (typically 100 to 300 μM),
 840 which stimulates respiration transiently on the basis of endogenous fuel substrates and phosphorylates
 841 only a small portion of the added ADP. State 2 is then obtained at a low respiratory activity limited by
 842 exhausted endogenous fuel substrate availability (**Table 3**). If addition of specific inhibitors of
 843 respiratory complexes—such as rotenone—does not cause a further decline of O₂ flux, State 2 is
 844 equivalent to the ROX state (See below.). If inhibition is observed, undefined endogenous fuel substrates
 845 are a confounding factor of pathway control, contributing to the effect of subsequently externally added
 846 substrates and inhibitors. In contrast to the original protocol, an alternative sequence of titration steps is
 847 frequently applied, in which the alternative 'State 2' has an entirely different meaning, when this second
 848 state is induced by addition of fuel substrate without ADP or ATP (LEAK-state; in contrast to State 2
 849 defined in **Table 1** as a ROX state). Some researchers have called this condition as "pseudostate 4"
 850 because it has no significant concentrations of adenine nucleotides and hence it is not a near-
 851 physiological condition, although it should be used for calculating the net OXPHOS-capacity, *P-L*.

852 **2.6.3. State 3** is the state stimulated by addition of fuel substrates while the ADP concentration
 853 is still high (**Table 3**) and supports coupled energy transformation through oxidative phosphorylation.
 854 'High ADP' is a concentration of ADP specifically selected to allow the measurement of State 3 to State
 855 4 transitions of isolated mitochondria in a closed respirometric chamber. Repeated ADP titration re-
 856 establishes State 3 at 'high ADP'. Starting at O₂ concentrations near air-saturation (193 or 238 μM O₂
 857 at 37 °C or 25 °C and sea level at 1 atm or 101.32 kPa, and an oxygen solubility of respiration medium
 858 at 0.92 times that of pure water; Forstner and Gnaiger 1983), the total ADP concentration added must
 859 be low enough (typically 100 to 300 μM) to allow phosphorylation to ATP at a coupled O₂ flux that
 860 does not lead to O₂ depletion during the transition to State 4. In contrast, kinetically-saturating ADP
 861 concentrations usually are 10-fold higher than 'high ADP', *e.g.*, 2.5 mM in isolated mitochondria. The

862 abbreviation State 3u is occasionally used in bioenergetics, to indicate the state of respiration after
 863 titration of an uncoupler, without sufficient emphasis on the fundamental difference between OXPHOS-
 864 capacity (*well-coupled* with an endogenous uncoupled component) and ET-capacity (*noncoupled*).

865 **2.6.4. State 4** is a LEAK-state that is obtained only if the mitochondrial preparation is intact and
 866 well-coupled. Depletion of ADP by phosphorylation to ATP causes a decline of O₂ flux in the transition
 867 from State 3 to State 4. Under the conditions of State 4, a maximum protonmotive force and high
 868 ATP/ADP ratio are maintained. The gradual decline of $Y_{P\gg/O_2}$ towards diminishing [ADP] at State 4 must
 869 be taken into account for calculation of $P\gg/O_2$ ratios (Gnaiger 2001). State 4 respiration, L_T (**Table 1**),
 870 reflects intrinsic proton leak and ATP hydrolysis activity. O₂ flux in State 4 is an overestimation of
 871 LEAK-respiration if the contaminating ATP hydrolysis activity recycles some ATP to ADP, $J_{P\ll}$, which
 872 stimulates respiration coupled to phosphorylation, $J_{P\gg} > 0$. Some degree of mechanical disruption and
 873 loss of mitochondrial integrity allows the exposed mitochondrial F-ATPases to hydrolyze the ATP
 874 synthesized by the fraction of coupled mitochondria. This can be tested by inhibition of the
 875 phosphorylation-pathway using oligomycin, ensuring that $J_{P\gg} = 0$ (State 4o). On the other hand, the State
 876 4 respiration reached after exhaustion of added ADP is a more physiological condition (*i.e.*, presence of
 877 ATP, ADP and even AMP). Sequential ADP titrations re-establish State 3, followed by State 3 to State
 878 4 transitions while sufficient O₂ is available. Anoxia may be reached, however, before exhaustion of
 879 ADP (State 5).

880 **2.6.5. State 5** is the state after exhaustion of O₂ in a closed respirometric chamber. Diffusion of
 881 O₂ from the surroundings into the aqueous solution may be a confounding factor preventing complete
 882 anoxia (Gnaiger 2001). Chance and Williams (1955) provide an alternative definition of State 5, which
 883 gives it the different meaning of ROX versus anoxia: ‘State 5 may be obtained by antimycin A treatment
 884 or by anaerobiosis’.

885 In **Table 3**, only States 3 and 4 are coupling control states, with the restriction that rates in State
 886 3 may be limited kinetically by non-saturating ADP concentrations.

887

888 2.7. Control and regulation

889

890 The terms metabolic *control* and *regulation* are frequently used synonymously, but are
 891 distinguished in metabolic control analysis: ‘We could understand the regulation as the mechanism that
 892 occurs when a system maintains some variable constant over time, in spite of fluctuations in external
 893 conditions (homeostasis of the internal state). On the other hand, metabolic control is the power to
 894 change the state of the metabolism in response to an external signal’ (Fell 1997). Respiratory control
 895 may be induced by experimental control signals that exert an influence on: (1) ATP demand and ADP
 896 phosphorylation-rate; (2) fuel substrate composition, pathway competition; (3) available amounts of
 897 substrates and O₂, *e.g.*, starvation and hypoxia; (4) the protonmotive force, redox states, flux–force
 898 relationships, coupling and efficiency; (5) Ca²⁺ and other ions including H⁺; (6) inhibitors, *e.g.*, nitric
 899 oxide or intermediary metabolites such as oxaloacetate; (7) signalling pathways and regulatory proteins,
 900 *e.g.*, insulin resistance, transcription factor hypoxia inducible factor 1.

901 Mechanisms of respiratory control and regulation include adjustments of: (1) enzyme activities
 902 by allosteric mechanisms and phosphorylation; (2) enzyme content, concentrations of cofactors and
 903 conserved moieties—such as adenylates, nicotinamide adenine dinucleotide [NAD⁺/NADH], coenzyme
 904 Q, cytochrome *c*; (3) metabolic channeling by supercomplexes; and (4) mitochondrial density (enzyme
 905 concentrations and membrane area) and morphology (cristae folding, fission and fusion). Mitochondria
 906 are targeted directly by hormones, *e.g.*, progesterone and glucacorticoids, which affect their energy
 907 metabolism (Lee *et al.* 2013; Gerö and Szabo 2016; Price and Dai 2016; Moreno *et al.* 2017).
 908 Evolutionary or acquired differences in the genetic and epigenetic basis of mitochondrial function (or
 909 dysfunction) between individuals; age; biological sex, and hormone concentrations; life style including
 910 exercise and nutrition; and environmental issues including thermal, atmospheric, toxic and
 911 pharmacological factors, exert an influence on all control mechanisms listed above. For reviews, see
 912 Brown 1992; Gnaiger 1993a, 2009; 2014; Paradies *et al.* 2014; Morrow *et al.* 2017.

913 Lack of control by a metabolic pathway, *e.g.*, phosphorylation-pathway, means that there will
 914 be no response to a variable activating it, *e.g.*, [ADP]. The reverse, however, is not true as the absence
 915 of a response to [ADP] does not exclude the phosphorylation-pathway from having some degree of
 916 control. The degree of control of a component of the OXPHOS-pathway on an output variable—such
 917 as O₂ flux, will in general be different from the degree of control on other outputs—such as

918 phosphorylation-flux or proton leak flux. Therefore, it is necessary to be specific as to which input and
919 output are under consideration (Fell 1997).

920 Respiratory control refers to the ability of mitochondria to adjust O₂ flux in response to external
921 control signals by engaging various mechanisms of control and regulation. Respiratory control is
922 monitored in a mitochondrial preparation under conditions defined as respiratory states, preferentially
923 under near-physiological conditions of temperature, pH and medium ionic composition, to generate data
924 of higher biological relevance. When phosphorylation of ADP to ATP is stimulated or depressed, an
925 increase or decrease is observed in electron transfer measured as O₂ flux in respiratory coupling states
926 of intact mitochondria ('controlled states' in the classical terminology of bioenergetics). Alternatively,
927 coupling of electron transfer with phosphorylation is diminished by uncouplers. The corresponding
928 coupling control state is characterized by a high respiratory rate without control by P» (noncoupled or
929 'uncontrolled state').

930
931

932 3. What is a rate?

933

934 The term *rate* is not adequately defined to be useful for reporting data. Normalization of 'rates'
935 leads to a diversity of formats. Application of common and defined units is required for direct transfer
936 of reported results into a database. The second [s] is the SI unit for the base quantity *time*. It is also the
937 standard time-unit used in solution chemical kinetics.

938 The inconsistency of the meanings of rate becomes apparent when considering Galileo Galilei's
939 famous principle, that 'bodies of different weight all fall at the same rate (have a constant acceleration)'
940 (Coopersmith 2010). A rate may be an extensive quantity, which is a *flow*, *I*, when expressed per object
941 (per number of cells or organisms) or per chamber (per system). 'System' is defined as the open or
942 closed chamber of the measuring device. A rate is a *flux*, *J*, when expressed as a size-specific quantity
943 (**Figure 6A; Box 2**).

944 • **Extensive quantities:** An extensive quantity increases proportionally with system size. For
945 example, mass and volume are extensive quantities. Flow is an extensive quantity. The
946 magnitude of an extensive quantity is completely additive for non-interacting subsystems.
947 The magnitude of these quantities depends on the extent or size of the system (Cohen *et al.*
948 2008).

949 • **Size-specific quantities:** 'The adjective *specific* before the name of an extensive quantity is
950 often used to mean *divided by mass*' (Cohen *et al.* 2008). In this system-paradigm, mass-
951 specific flux is flow divided by mass of the system (the total mass of everything within the
952 measuring chamber or reactor). Rates are frequently expressed as volume-specific flux. A
953 mass-specific or volume-specific quantity is independent of the extent of non-interacting
954 homogenous subsystems. Tissue-specific quantities (related to the *sample* in contrast to the
955 *system*) are of fundamental interest in the field of comparative mitochondrial physiology,
956 where *specific* refers to the *type of the sample* rather than *mass of the system*. The term
957 *specific*, therefore, must be clarified; *sample-specific*, *e.g.*, muscle mass-specific
958 normalization, is distinguished from *system-specific* quantities (mass or volume; **Figure 6**).

959 • **Intensive quantities:** In contrast to size-specific properties, forces are intensive quantities
960 defined as the change of an extensive quantity per advancement of an energy transformation
961 (Gnaiger 1993b).

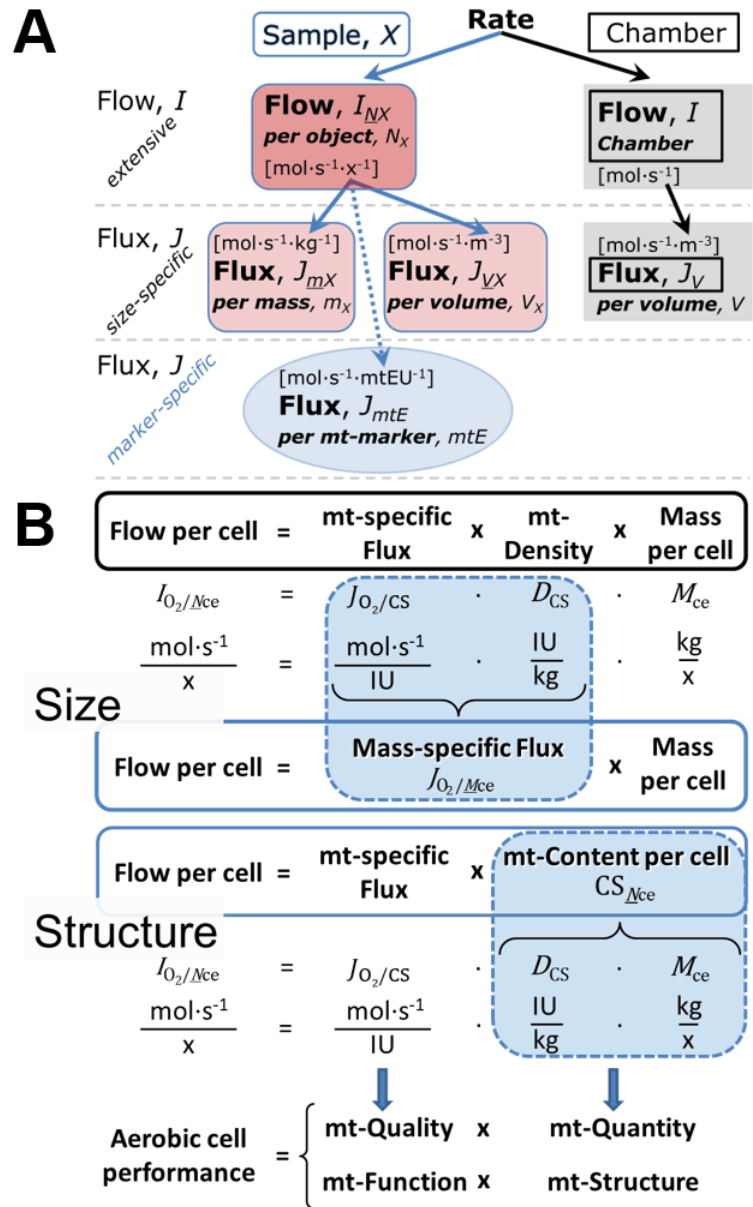
962 • N_X and m_X indicate the number format and mass format, respectively, for expressing the
963 quantity of a sample *X*. When different formats are indicated in symbols of derived quantities,
964 the format (\underline{N} , \underline{m}) is shown as a subscript (*underlined italic*), as in $I_{O_2/\underline{N}X}$ and $J_{O_2/\underline{m}X}$. Oxygen
965 flow and flux are expressed in the molar format, n_{O_2} [mol], but in the volume format, V_{O_2} [m³]
966 in ergometry. For mass-specific flux these formats can be distinguished as $J_{\underline{n}O_2/\underline{m}X}$ and $J_{V_{O_2}/\underline{m}X}$,
967 respectively. Further examples are given in **Figure 6** and **Table 4**.

968

969 **Figure 6. Flow and flux, and**
 970 **normalization in structure-**
 971 **function analysis**

972 (A) When expressing metabolic
 973 ‘rate’ measured in a chamber, a
 974 fundamental distinction is made
 975 between relating the rate to the
 976 experimental sample (left) or
 977 chamber (right). The different
 978 meanings of rate need to be
 979 specified by the chosen
 980 normalization. Left: Results are
 981 expressed as mass-specific flux, J_{mX} ,
 982 per mg protein, dry or wet mass.
 983 Cell volume, V_{ce} , may be used for
 984 normalization (volume-specific
 985 flux, J_{Vce}). Right: Flow per chamber,
 986 I , or flux per chamber volume, J_V ,
 987 are merely reported for
 988 methodological reasons.

989 (B) O_2 flow per cell, $I_{O_2/Nce}$, is the
 990 product of mitochondria-specific
 991 flux, mt-density and mass per cell.
 992 Unstructured analysis: performance
 993 is the product of mass-specific flux,
 994 $J_{O_2/MX}$ [$\text{mol}\cdot\text{s}^{-1}\cdot\text{kg}^{-1}$], and size
 995 (mass per cell). Structured analysis:
 996 performance is the product of
 997 mitochondrial function (mt-specific
 998 flux) and structure (mt-content).
 999 Modified from Gnaiger (2014). For
 1000 further details see **Table 4**.



1006 **Box 2: Metabolic flows and fluxes: vectoral, vectorial, and scalar**

1007
 1008 In a generalization of electrical terms, flow as an extensive quantity (I ; per system) is
 1009 distinguished from flux as a size-specific quantity (J ; per system size). *Flows*, I_{tr} , are defined for all
 1010 transformations as extensive quantities. Electric charge per unit time is electric flow or current, $I_{el} =$
 1011 $dQ_{el} \cdot dt^{-1}$ [$A \equiv C \cdot s^{-1}$]. When dividing I_{el} by size of the system (cross-sectional area of a ‘wire’), we obtain
 1012 flux as a size-specific quantity, which is the current density (surface-density of flow) perpendicular to
 1013 the direction of flux, $J_{el} = I_{el} \cdot A^{-1}$ [$A \cdot m^{-2}$] (Cohen et al. 2008). Fluxes with *spatial* geometric direction and
 1014 magnitude are *vectors*. Vector and scalar *fluxes* are related to flows as $J_{tr} = I_{tr} \cdot A^{-1}$ [$\text{mol}\cdot\text{s}^{-1}\cdot\text{m}^{-2}$] and $J_{tr} =$
 1015 $I_{tr} \cdot V^{-1}$ [$\text{mol}\cdot\text{s}^{-1}\cdot\text{m}^{-3}$], expressing flux as an area-specific vector or volume-specific vectorial or scalar
 1016 quantity, respectively (Gnaiger 1993b). We use the metre–kilogram–second–ampere (MKSA)
 1017 international system of units (SI) for general cases ([m], [kg], [s] and [A]), with decimal SI prefixes for
 1018 specific applications (**Table 4**).

1019 We suggest to define: (1) *vectoral* fluxes, which are translocations as functions of *gradients* with
 1020 direction in geometric space in continuous systems; (2) *vectorial* fluxes, which describe translocations
 1021 in discontinuous systems and are restricted to information on *compartmental differences*
 1022 (transmembrane proton flux); and (3) *scalar* fluxes, which are transformations in a *homogenous* system
 1023 (catabolic O_2 flux, J_{kO_2}).

1024 **4. Normalization of rate per sample**

1025

1026 The challenges of measuring mitochondrial respiratory flux are matched by those of
 1027 normalization. Normalization (**Table 4**) is guided by physicochemical principles, methodological
 1028 considerations, and conceptual strategies (**Figure 6**).

1029

1030 **Table 4. Sample concentrations and normalization of flux.**

1031

| Expression | Symbol | Definition | Unit | Notes |
|--|---------------|--|---|-------|
| Sample | | | | |
| identity of sample | X | object: cell, tissue, animal, patient | | |
| number of sample entities X | N_X | number of objects | x | 1 |
| mass of sample X | m_X | | kg | 2 |
| mass of object X | M_X | $M_X = m_X \cdot N_X^{-1}$ | $\text{kg} \cdot \text{x}^{-1}$ | 2 |
| Mitochondria | | | | |
| mitochondria | mt | $X = \text{mt}$ | | |
| amount of mt-elementary components | mtE | quantity of mt-marker | mtEU | |
| Concentrations | | | | |
| object number concentration | C_{NX} | $C_{NX} = N_X \cdot V^{-1}$ | $\text{x} \cdot \text{m}^{-3}$ | 3 |
| sample mass concentration | C_{mX} | $C_{mX} = m_X \cdot V^{-1}$ | $\text{kg} \cdot \text{m}^{-3}$ | |
| mitochondrial concentration | C_{mtE} | $C_{mtE} = mtE \cdot V^{-1}$ | $\text{mtEU} \cdot \text{m}^{-3}$ | 4 |
| specific mitochondrial density | D_{mtE} | $D_{mtE} = mtE \cdot m_X^{-1}$ | $\text{mtEU} \cdot \text{kg}^{-1}$ | 5 |
| mitochondrial content, mtE per object X | mtE_{NX} | $mtE_{NX} = mtE \cdot N_X^{-1}$ | $\text{mtEU} \cdot \text{x}^{-1}$ | 6 |
| O₂ flow and flux | | | | |
| flow, system | I_{O_2} | internal flow | $\text{mol} \cdot \text{s}^{-1}$ | 7 |
| volume-specific flux | J_{V,O_2} | $J_{V,O_2} = I_{O_2} \cdot V^{-1}$ | $\text{mol} \cdot \text{s}^{-1} \cdot \text{m}^{-3}$ | 8 |
| flow per object X | $I_{O_2/NX}$ | $I_{O_2/NX} = J_{V,O_2} \cdot C_{NX}^{-1}$ | $\text{mol} \cdot \text{s}^{-1} \cdot \text{x}^{-1}$ | 9 |
| mass-specific flux | $J_{O_2/mX}$ | $J_{O_2/mX} = J_{V,O_2} \cdot C_{mX}^{-1}$ | $\text{mol} \cdot \text{s}^{-1} \cdot \text{kg}^{-1}$ | 10 |
| mt-marker-specific flux | $J_{O_2/mtE}$ | $J_{O_2/mtE} = J_{V,O_2} \cdot C_{mtE}^{-1}$ | $\text{mol} \cdot \text{s}^{-1} \cdot \text{mtEU}^{-1}$ | 11 |

1032

1033 1 The unit x for a number is not used by IUPAC. To avoid confusion, the units [$\text{kg} \cdot \text{x}^{-1}$] and [kg]
 1034 distinguish the mass per object from the mass of a sample that may contain any number of objects.
 1035 Similarly, the units for flow per system *versus* flow per object are [$\text{mol} \cdot \text{s}^{-1}$] (Note 8) and [$\text{mol} \cdot \text{s}^{-1} \cdot \text{x}^{-1}$]
 1036 (Note 10).

1037

1038 2 Units are given in the MKSA system (**Box 2**). The *SI* prefix k is used for the *SI* base unit of mass (kg
 1039 = 1,000 g). In praxis, various *SI* prefixes are used for convenience, to make numbers easily readable,
 1040 e.g., 1 mg tissue, cell or mitochondrial mass instead of 0.000001 kg.

1041

1042 3 In case of cells (sample $X = \text{cells}$), the object number concentration is $C_{N_{ce}} = N_{ce} \cdot V^{-1}$, and volume
 1043 may be expressed in [$\text{dm}^3 \equiv \text{L}$] or [$\text{cm}^3 = \text{mL}$]. See **Table 5** for different object types.

1044

1045 4 mt-concentration is an experimental variable, dependent on sample concentration: (1) $C_{mtE} = mtE \cdot V^{-1}$;

1046

1047 (2) $C_{mtE} = mtE_{NX} \cdot C_{NX}$; (3) $C_{mtE} = C_{mX} \cdot D_{mtE}$.

1048

1049 5 If the amount of mitochondria, mtE , is expressed as mitochondrial mass, then D_{mtE} is the mass
 fraction of mitochondria in the sample. If mtE is expressed as mitochondrial volume, V_{mt} , and the
 mass of sample, m_X , is replaced by volume of sample, V_X , then D_{mtE} is the volume fraction of
 mitochondria in the sample.

1047

1048 6 $mtE_{NX} = mtE \cdot N_X^{-1} = C_{mtE} \cdot C_{NX}^{-1}$.

1049

1049 7 O₂ can be replaced by other chemicals to study different reactions, e.g., ATP, H₂O₂, or vesicular
 compartmental translocations, e.g., Ca²⁺.

- 1050 8 I_{O_2} and V are defined per instrument chamber as a system of constant volume (and constant
 1051 temperature), which may be closed or open. I_{O_2} is abbreviated for I_{rO_2} , *i.e.*, the metabolic or internal
 1052 O_2 flow of the chemical reaction r in which O_2 is consumed, hence the negative stoichiometric
 1053 number, $v_{O_2} = -1$. $I_{rO_2} = d_r n_{O_2} / dt \cdot v_{O_2}^{-1}$. If r includes all chemical reactions in which O_2 participates, then
 1054 $d_r n_{O_2} = dn_{O_2} - d_e n_{O_2}$, where dn_{O_2} is the change in the amount of O_2 in the instrument chamber and $d_e n_{O_2}$
 1055 is the amount of O_2 added externally to the system. At steady state, by definition $dn_{O_2} = 0$, hence $d_r n_{O_2}$
 1056 $= -d_e n_{O_2}$.
- 1057 9 J_{V,O_2} is an experimental variable, expressed per volume of the instrument chamber.
- 1058 10 $I_{O_2/\underline{NX}}$ is a physiological variable, depending on the size of entity X .
- 1059 11 There are many ways to normalize for a mitochondrial marker, that are used in different experimental
 1060 approaches: (1) $J_{O_2/mtE} = J_{V,O_2} \cdot C_{mtE}^{-1}$; (2) $J_{O_2/mtE} = J_{V,O_2} \cdot C_{mX}^{-1} \cdot D_{mtE}^{-1} = J_{O_2/mX} \cdot D_{mtE}^{-1}$; (3) $J_{O_2/mtE} =$
 1061 $J_{V,O_2} \cdot C_{NX}^{-1} \cdot mtE_{NX}^{-1} = I_{O_2/\underline{NX}} \cdot mtE_{NX}^{-1}$; (4) $J_{O_2/mtE} = I_{O_2} \cdot mtE^{-1}$. The mt-elementary unit [mtE] varies depending
 1062 on the mt-marker.

1063 **Table 5. Sample types, X , abbreviations, and quantification.**

| Identity of sample | X | N_X | Mass ^a | Volume | mt-Marker |
|---------------------------|------|-----------|-------------------|-------------------|--------------|
| mitochondrial preparation | | [x] | [kg] | [m ³] | [mtE] |
| isolated mitochondria | imt | | m_{mt} | V_{mt} | mtE |
| tissue homogenate | thom | | m_{thom} | | mtE_{thom} |
| permeabilized tissue | pti | | m_{pti} | | mtE_{pti} |
| permeabilized fibre | pfi | | m_{pfi} | | mtE_{pfi} |
| permeabilized cell | pce | N_{pce} | M_{pce} | V_{pce} | mtE_{pce} |
| cells ^b | ce | N_{ce} | M_{ce} | V_{ce} | mtE_{ce} |
| intact cell, viable cell | vce | N_{vce} | M_{vce} | V_{vce} | |
| dead cell | dce | N_{dce} | M_{dce} | V_{dce} | |
| organism | org | N_{org} | M_{org} | V_{org} | |

1065 ^a Instead of mass, the wet weight or dry weight is frequently stated, W_w or W_d . m_X is
 1066 mass of the sample [kg], M_X is mass of the object [kg·x⁻¹] (**Table 4**).

1067 ^b Total cell count, $N_{ce} = N_{vce} + N_{dce}$

1068 4.1. Flow: per object

1071 **4.1.1. Number concentration, C_{NX} :** Normalization per sample concentration is routinely required
 1072 to report respiratory data. C_{NX} is the experimental number concentration of sample X . In the case of
 1073 animals, *e.g.*, nematodes, $C_{NX} = N_X/V$ [x·L⁻¹], where N_X is the number of organisms in the chamber.
 1074 Similarly, the number of cells per chamber volume is the number concentration of permeabilized or
 1075 intact cells $C_{Nce} = N_{ce}/V$ [x·L⁻¹], where N_{ce} is the number of cells in the chamber (**Table 4**).

1076 **4.1.2. Flow per object, $I_{O_2/\underline{NX}}$:** O_2 flow per cell is calculated from volume-specific O_2 flux, J_{V,O_2}
 1077 [nmol·s⁻¹·L⁻¹] (per V of the measurement chamber [L]), divided by the number concentration of cells.
 1078 The total cell count is the sum of viable and dead cells, $N_{ce} = N_{vce} + N_{dce}$ (**Table 5**). The cell viability
 1079 index, $VI = N_{vce}/N_{ce}$, is the ratio of viable cells (N_{vce} ; before experimental permeabilization) per total cell
 1080 count. After experimental permeabilization, all cells are permeabilized, $N_{pce} = N_{ce}$. The cell viability
 1081 index can be used to normalize respiration for the number of cells that have been viable before
 1082 experimental permeabilization, $I_{O_2/\underline{Nvce}} = I_{O_2/\underline{Nce}}/VI$, considering that mitochondrial respiratory
 1083 dysfunction in dead cells should be eliminated as a confounding factor.

1084 The complexity changes when the object is a whole organism studied as an experimental model.
 1085 The scaling law in respiratory physiology reveals a strong interaction between O_2 flow and individual
 1086 body mass, since *basal* metabolic rate (flow) does not increase linearly with body mass, whereas
 1087 *maximum* mass-specific O_2 flux, \dot{V}_{O_2max} or \dot{V}_{O_2peak} , is approximately constant across a large range of
 1088 individual body mass (Weibel and Hoppeler 2005), with individuals, breeds, and species deviating
 1089 substantially from this relationship. \dot{V}_{O_2peak} of human endurance athletes is 60 to 80 mL $O_2 \cdot \text{min}^{-1} \cdot \text{kg}^{-1}$
 1090 body mass, converted to $J_{O_2peak/Morg}$ of 45 to 60 nmol·s⁻¹·g⁻¹ (Gnaiger 2014; **Table 6**).

1091
 1092

4.2. Size-specific flux: per sample size

4.2.1. Sample concentration, C_{mX} : Considering permeabilized tissue, homogenate or cells as the sample, X , the sample mass is m_X [mg], which is frequently measured as wet or dry weight, W_w or W_d [mg], respectively, or as amount of protein, m_{Protein} . The sample concentration is the mass of the subsample per volume of the measurement chamber, $C_{mX} = m_X/V$ [$\text{g}\cdot\text{L}^{-1} = \text{mg}\cdot\text{mL}^{-1}$]. X is the type of sample—isolated mitochondria, tissue homogenate, permeabilized fibres or cells (**Table 5**).

4.2.2. Size-specific flux: Cellular O_2 flow can be compared between cells of identical size. To take into account changes and differences in cell size, normalization is required to obtain cell size-specific or mitochondrial marker-specific O_2 flux (Renner *et al.* 2003).

- **Mass-specific flux, $J_{\text{O}_2/mX}$ [$\text{mol}\cdot\text{s}^{-1}\cdot\text{kg}^{-1}$]:** Mass-specific flux is obtained by expressing respiration per mass of sample, m_X [mg]. Flow per cell is divided by mass per cell, $J_{\text{O}_2/mce} = I_{\text{O}_2/Nce}/M_{Nce}$. Or chamber volume-specific flux, J_{V,O_2} , is divided by mass concentration of X in the chamber, $J_{\text{O}_2/mX} = J_{V,\text{O}_2}/C_{mX}$.
- **Cell volume-specific flux, $J_{\text{O}_2/VX}$ [$\text{mol}\cdot\text{s}^{-1}\cdot\text{m}^{-3}$]:** Sample volume-specific flux is obtained by expressing respiration per volume of sample. For example, in the case of using cells as sample will be the volume of cells added to the chamber (**Figure 6**).

If size-specific O_2 flux is constant and independent of sample size, then there is no interaction between the subsystems. For example, a 1.5 mg and a 3.0 mg muscle sample respire at identical mass-specific flux. Mass-specific O_2 flux, however, may change with the mass of a tissue sample, cells or isolated mitochondria in the measuring chamber, in which the nature of the interaction becomes an issue. Therefore, cell density must be optimized, particularly in experiments carried out in wells, considering the confluency of the cell monolayer or clumps of cells (Salabei *et al.* 2014).

4.3. Marker-specific flux: per mitochondrial content

Tissues can contain multiple cell populations that may have distinct mitochondrial subtypes. Mitochondria undergo dynamic fission and fusion cycles, and can exist in multiple stages and sizes that may be altered by a range of factors. The isolation of mitochondria (often achieved through differential centrifugation) can therefore yield a subsample of the mitochondrial types present in a tissue, depending on the isolation protocols utilized (*e.g.*, centrifugation speed). This possible bias should be taken into account when planning experiments using isolated mitochondria. Different sizes of mitochondria are enriched at specific centrifugation speeds, which can be used strategically for isolation of mitochondrial subpopulations.

Part of the mitochondrial content of a tissue is lost during preparation of isolated mitochondria. The fraction of isolated mitochondria obtained from a tissue sample is expressed as mitochondrial recovery. At a high mitochondrial recovery the fraction of isolated mitochondria is more representative of the total mitochondrial population than in preparations characterized by low recovery. Determination of the mitochondrial recovery and yield is based on measurement of the concentration of a mitochondrial marker in the stock of isolated mitochondria, $C_{mtE,stock}$, and crude tissue homogenate, $C_{mtE,thom}$, which simultaneously provides information on the specific mitochondrial density in the sample, D_{mtE} (**Table 4**).

When discussing concepts on normalization, it is essential to consider the question of the study. If the study aims at comparing tissue performance—such as the effects of a treatment on a specific tissue, then normalization for tissue mass or protein content is appropriate. However, if the aim is to find differences on mitochondrial function independent of mitochondrial density (**Table 4**), then normalization to a mitochondrial marker is imperative (**Figure 6**). One cannot assume that quantitative changes in various markers—such as mitochondrial proteins—necessarily occur in parallel with one another. It should be established that the marker chosen is not selectively altered by the performed treatment. In conclusion, the normalization must reflect the question under investigation to reach a satisfying answer. On the other hand, the goal of comparing results across projects and institutions requires standardization on normalization for entry into a databank.

4.3.1. Mitochondrial concentration, C_{mtE} , and mitochondrial markers: Mitochondrial organelles comprise a dynamic cellular reticulum in various states of fusion and fission. Hence, the definition of an "amount" of mitochondria is often misconceived: mitochondria cannot be counted

1149 reliably as a number of occurring elementary components. Therefore, quantification of the "amount" of
 1150 mitochondria depends on the measurement of chosen mitochondrial markers. 'Mitochondria are the
 1151 structural and functional elementary units of cell respiration' (Gnaiger 2014). The quantity of a
 1152 mitochondrial marker can reflect the amount of *mitochondrial elementary components*, mtE , expressed
 1153 in various mitochondrial elementary units [mtEU] specific for each measured mt-marker (**Table 4**).
 1154 However, since mitochondrial quality may change in response to stimuli—particularly in mitochondrial
 1155 dysfunction (Campos *et al.* 2017) and after exercise training (Pesta *et al.* 2011) and during aging (Daum
 1156 *et al.* 2013)—some markers can vary while others are unchanged: (1) Mitochondrial volume and
 1157 membrane area are structural markers, whereas mitochondrial protein mass is commonly used as a
 1158 marker for isolated mitochondria. (2) Molecular and enzymatic mitochondrial markers (amounts or
 1159 activities) can be selected as matrix markers, *e.g.*, citrate synthase activity, mtDNA; mtIM-markers, *e.g.*,
 1160 cytochrome *c* oxidase activity, aa_3 content, cardiolipin, or mtOM-markers, *e.g.*, the voltage-dependent
 1161 anion channel (VDAC), TOM20. (3) Extending the measurement of mitochondrial marker enzyme
 1162 activity to mitochondrial pathway capacity, ET- or OXPHOS-capacity can be considered as an
 1163 integrative functional mitochondrial marker.

1164 Depending on the type of mitochondrial marker, the mitochondrial elementary component, mtE ,
 1165 is expressed in marker-specific units. Mitochondrial concentration in the measurement chamber and the
 1166 tissue of origin are quantified as (1) a quantity for normalization in functional analyses, C_{mtE} , and (2) a
 1167 physiological output that is the result of mitochondrial biogenesis and degradation, D_{mtE} , respectively
 1168 (**Table 4**). It is recommended, therefore, to distinguish *experimental mitochondrial concentration*, C_{mtE}
 1169 = mtE/V and *physiological mitochondrial density*, $D_{mtE} = mtE/m_X$. Then mitochondrial density is the
 1170 amount of mitochondrial elementary components per mass of tissue, which is a biological variable
 1171 (**Figure 6**). The experimental variable is mitochondrial density multiplied by sample mass concentration
 1172 in the measuring chamber, $C_{mtE} = D_{mtE} \cdot C_{mX}$, or mitochondrial content multiplied by sample number
 1173 concentration, $C_{mtE} = mtE_X \cdot C_{NX}$ (**Table 4**).

1174 **4.3.2. mt-Marker-specific flux, $J_{O_2/mtE}$:** Volume-specific metabolic O_2 flux depends on: (1) the
 1175 sample concentration in the volume of the instrument chamber, C_{mX} , or C_{NX} ; (2) the mitochondrial
 1176 density in the sample, $D_{mtE} = mtE/m_X$ or $mtE_X = mtE/N_X$; and (3) the specific mitochondrial activity or
 1177 performance per elementary mitochondrial unit, $J_{O_2/mtE} = J_{V,O_2}/C_{mtE}$ [$mol \cdot s^{-1} \cdot mtEU^{-1}$] (**Table 4**).
 1178 Obviously, the numerical results for $J_{O_2/mtE}$ vary with the type of mitochondrial marker chosen for
 1179 measurement of mtE and $C_{mtE} = mtE/V$ [$mtEU \cdot m^{-3}$].

1180 Different methods are implicated in the quantification of mitochondrial markers and have
 1181 different strengths. Some problems are common for all mitochondrial markers, mtE : (1) Accuracy of
 1182 measurement is crucial, since even a highly accurate and reproducible measurement of O_2 flux results
 1183 in an inaccurate and noisy expression if normalized by a biased and noisy measurement of a
 1184 mitochondrial marker. This problem is acute in mitochondrial respiration because the denominators used
 1185 (the mitochondrial markers) are often small moieties of which accurate and precise determination is
 1186 difficult. This problem can be avoided when O_2 fluxes measured in substrate-uncoupler-inhibitor
 1187 titration protocols are normalized for flux in a defined respiratory reference state, which is used as an
 1188 *internal* marker and yields flux control ratios, $FCRs$. $FCRs$ are independent of externally measured
 1189 markers and, therefore, are statistically robust, considering the limitations of ratios in general (Jasienski
 1190 and Bazzaz 1999). $FCRs$ indicate qualitative changes of mitochondrial respiratory control, with highest
 1191 quantitative resolution, separating the effect of mitochondrial density or concentration on $J_{O_2/mX}$ and
 1192 $J_{O_2/NX}$ from that of function per elementary mitochondrial marker, $J_{O_2/mtE}$ (Pesta *et al.* 2011; Gnaiger
 1193 2014). (2) If mitochondrial quality does not change and only the amount of mitochondria varies as a
 1194 determinant of mass-specific flux, any marker is equally qualified in principle; then in practice selection
 1195 of the optimum marker depends only on the accuracy and precision of measurement of the mitochondrial
 1196 marker. (3) If mitochondrial flux control ratios change, then there may not be any best mitochondrial
 1197 marker. In general, measurement of multiple mitochondrial markers enables a comparison and
 1198 evaluation of normalization for a variety of mitochondrial markers. Particularly during postnatal
 1199 development, the activity of marker enzymes—such as cytochrome *c* oxidase and citrate synthase—
 1200 follows different time courses (Drahota *et al.* 2004). Evaluation of mitochondrial markers in healthy
 1201 controls is insufficient for providing guidelines for application in the diagnosis of pathological states
 1202 and specific treatments.

1203 In line with the concept of the respiratory control ratio (Chance and Williams 1955a), the most
 1204 readily used normalization is that of flux control ratios and flux control factors (Gnaiger 2014). Selection

1205 of the state of maximum flux in a protocol as the reference state has the advantages of: (1) internal
 1206 normalization; (2) statistically validated linearization of the response in the range of 0 to 1; and (3)
 1207 consideration of maximum flux for integrating a large number of elementary steps in the OXPHOS- or
 1208 ET-pathways. This reduces the risk of selecting a functional marker that is specifically altered by the
 1209 treatment or pathology, yet increases the chance that the highly integrative pathway is disproportionately
 1210 affected, *e.g.*, the OXPHOS- rather than ET-pathway in case of an enzymatic defect in the
 1211 phosphorylation-pathway. In this case, additional information can be obtained by reporting flux control
 1212 ratios based on a reference state which indicates stable tissue-mass specific flux.

1213 Stereological determination of mitochondrial content via two-dimensional transmission electron
 1214 microscopy can have limitations due to the dynamics of mitochondrial size (Meinild Lundby *et al.*
 1215 2017). Accurate determination of three-dimensional volume by two-dimensional microscopy can be
 1216 both time consuming and statistically challenging (Larsen *et al.* 2012).

1217 The validity of using mitochondrial marker enzymes (citrate synthase activity, CI to CIV amount
 1218 or activity) for normalization of flux is limited in part by the same factors that apply to flux control
 1219 ratios. Strong correlations between various mitochondrial markers and citrate synthase activity
 1220 (Reichmann *et al.* 1985; Boushel *et al.* 2007; Mogensen *et al.* 2007) are expected in a specific tissue of
 1221 healthy persons and in disease states not specifically targeting citrate synthase. Citrate synthase activity
 1222 is acutely modifiable by exercise (Tonkonogi *et al.* 1997; Leek *et al.* 2001). Evaluation of mitochondrial
 1223 markers related to a selected age and sex cohort cannot be extrapolated to provide recommendations for
 1224 normalization in respirometric diagnosis of disease, in different states of development and ageing,
 1225 different cell types, tissues, and species. mtDNA normalized to nDNA via qPCR is correlated to
 1226 functional mitochondrial markers including OXPHOS- and ET-capacity in some cases (Puntschart *et al.*
 1227 1995; Wang *et al.* 1999; Menshikova *et al.* 2006; Boushel *et al.* 2007; Ehinger *et al.* 2015), but lack of
 1228 such correlations have been reported (Menshikova *et al.* 2005; Schultz and Wiesner 2000; Pesta *et al.*
 1229 2011). Several studies indicate a strong correlation between cardiolipin content and increase in
 1230 mitochondrial function with exercise (Menshikova *et al.* 2005; Menshikova *et al.* 2007; Larsen *et al.*
 1231 2012; Faber *et al.* 2014), but it has not been evaluated as a general mitochondrial biomarker in disease.
 1232 With no single best mitochondrial marker, a good strategy is to quantify several different biomarkers to
 1233 minimize the decorrelating effects caused by diseases, treatments, or other factors. Determination of
 1234 multiple markers, particularly a matrix marker and a marker from the mtIM, allows tracking changes in
 1235 mitochondrial quality defined by their ratio.

1236
 1237

1238 5. Normalization of rate per system

1239

1240 5.1. Flow: per chamber

1241

1242 The experimental system (experimental chamber) is part of the measurement instrument,
 1243 separated from the environment as an isolated, closed, open, isothermal or non-isothermal system
 1244 (Table 4). Reporting O₂ flows per respiratory chamber, I_{O_2} [nmol·s⁻¹], restricts the analysis to intra-
 1245 experimental comparison of relative differences.

1246

1247 5.2. Flux: per chamber volume

1248

1249 **5.2.1. System-specific flux, J_{V,O_2} :** We distinguish between (1) the *system* with volume V and mass
 1250 m defined by the system boundaries, and (2) the *sample* or *objects* with volume V_X and mass m_X that are
 1251 enclosed in the experimental chamber (Figure 6). Metabolic O₂ flow per object, I_{O_2/N_X} , is the total O₂
 1252 flow in the system divided by the number of objects, N_X , in the system. I_{O_2/N_X} increases as the mass of
 1253 the object is increased. Sample mass-specific O₂ flux, J_{O_2/m_X} should be independent of the mass of the
 1254 sample studied in the instrument chamber, but system volume-specific O₂ flux, J_{V,O_2} (per volume of the
 1255 instrument chamber), increases in proportion to the mass of the sample in the chamber. Whereas J_{V,O_2}
 1256 depends on mass-concentration of the sample in the chamber, it should be independent of the chamber
 1257 (system) volume at constant sample mass. There are practical limitations to increase the mass-
 1258 concentration of the sample in the chamber, when one is concerned about crowding effects and
 1259 instrumental time resolution.

5.2.2. Advancement per volume: When the reactor volume does not change during the reaction, which is typical for liquid phase reactions, the volume-specific *flux of a chemical reaction* r is the time derivative of the advancement of the reaction per unit volume, $J_{V,rB} = d_{t,r} \xi_B / dt \cdot V^{-1}$ [(mol·s⁻¹)·L⁻¹]. The *rate of concentration change* is dc_B/dt [(mol·L⁻¹)·s⁻¹], where concentration is $c_B = n_B/V$. There is a difference between (1) J_{V,rO_2} [mol·s⁻¹·L⁻¹] and (2) rate of concentration change [mol·L⁻¹·s⁻¹]. These merge to a single expression only in closed systems. In open systems, internal transformations (catabolic flux, O₂ consumption) are distinguished from external flux (such as O₂ supply). External fluxes of all substances are zero in closed systems. In a closed chamber O₂ consumption (internal flux of catabolic reactions k), I_{kO_2} [pmol·s⁻¹], causes a decline of the amount of O₂ in the system, n_{O_2} [nmol]. Normalization of these quantities for the volume of the system, V [L ≡ dm³], yields volume-specific O₂ flux, $J_{V,kO_2} = I_{kO_2}/V$ [nmol·s⁻¹·L⁻¹], and O₂ concentration, [O₂] or $c_{O_2} = n_{O_2}/V$ [μmol·L⁻¹ = μM = nmol·mL⁻¹]. Instrumental background O₂ flux is due to external flux into a non-ideal closed respirometer; then total volume-specific flux has to be corrected for instrumental background O₂ flux—O₂ diffusion into or out of the instrumental chamber. J_{V,kO_2} is relevant mainly for methodological reasons and should be compared with the accuracy of instrumental resolution of background-corrected flux, *e.g.*, ±1 nmol·s⁻¹·L⁻¹ (Gnaiger 2001). ‘Metabolic’ or catabolic indicates O₂ flux, J_{kO_2} , corrected for: (1) instrumental background O₂ flux; (2) chemical background O₂ flux due to autoxidation of chemical components added to the incubation medium; and (3) *Rox* for O₂-consuming side reactions unrelated to the catabolic pathway k .

6. Conversion of units

Many different units have been used to report the O₂ consumption rate, OCR (Table 6). SI base units provide the common reference to introduce the theoretical principles (Figure 6), and are used with appropriately chosen *SI* prefixes to express numerical data in the most practical format, with an effort towards unification within specific areas of application (Table 7). Reporting data in *SI* units—including the mole [mol], coulomb [C], joule [J], and second [s]—should be encouraged, particularly by journals which propose the use of *SI* units.

Table 6. Conversion of various formats and units used in respirometry and ergometry. e^- is the number of electrons or reducing equivalents. z_B is the charge number of entity B.

| Format | 1 Unit | | Multiplication factor | <i>SI</i> -unit | Notes |
|------------------------------------|---|-------------------|-----------------------|--------------------------------------|-------|
| \underline{n} | ng.atom O·s ⁻¹ | (2 e^-) | 0.5 | nmol O ₂ ·s ⁻¹ | |
| \underline{n} | ng.atom O·min ⁻¹ | (2 e^-) | 8.33 | pmol O ₂ ·s ⁻¹ | |
| \underline{n} | natom O·min ⁻¹ | (2 e^-) | 8.33 | pmol O ₂ ·s ⁻¹ | |
| \underline{n} | nmol O ₂ ·min ⁻¹ | (4 e^-) | 16.67 | pmol O ₂ ·s ⁻¹ | |
| \underline{n} | nmol O ₂ ·h ⁻¹ | (4 e^-) | 0.2778 | pmol O ₂ ·s ⁻¹ | |
| \underline{V} to \underline{n} | mL O ₂ ·min ⁻¹ at STPD ^a | | 0.744 | μmol O ₂ ·s ⁻¹ | 1 |
| \underline{e} to \underline{n} | W = J/s at -470 kJ/mol O ₂ | | -2.128 | μmol O ₂ ·s ⁻¹ | |
| \underline{e} to \underline{n} | mA = mC·s ⁻¹ | ($z_{H^+} = 1$) | 10.36 | nmol H ⁺ ·s ⁻¹ | 2 |
| \underline{e} to \underline{n} | mA = mC·s ⁻¹ | ($z_{O_2} = 4$) | 2.59 | nmol O ₂ ·s ⁻¹ | 2 |
| \underline{n} to \underline{e} | nmol H ⁺ ·s ⁻¹ | ($z_{H^+} = 1$) | 0.09649 | mA | 3 |
| \underline{n} to \underline{e} | nmol O ₂ ·s ⁻¹ | ($z_{O_2} = 4$) | 0.38594 | mA | 3 |

1 At standard temperature and pressure dry (STPD: 0 °C = 273.15 K and 1 atm = 101.325 kPa = 760 mmHg), the molar volume of an ideal gas, V_m , and V_{m,O_2} is 22.414 and 22.392 L·mol⁻¹, respectively. Rounded to three decimal places, both values yield the conversion factor of 0.744. For comparison at normal temperature and pressure dry (NTPD: 20 °C), V_{m,O_2} is 24.038 L·mol⁻¹. Note that the *SI* standard pressure is 100 kPa.

2 The multiplication factor is $10^6/(z_B \cdot F)$.

3 The multiplication factor is $z_B \cdot F/10^6$.

1299

Table 7. Conversion of units with preservation of numerical values.

| Name | Frequently used unit | Equivalent unit | Notes |
|--|---|---|-------|
| volume-specific flux, J_{V,O_2} | $\text{pmol}\cdot\text{s}^{-1}\cdot\text{mL}^{-1}$ $\text{mmol}\cdot\text{s}^{-1}\cdot\text{L}^{-1}$ | $\text{nmol}\cdot\text{s}^{-1}\cdot\text{L}^{-1}$ $\text{mol}\cdot\text{s}^{-1}\cdot\text{m}^{-3}$ | 1 |
| cell-specific flow, $I_{O_2/\text{cell}}$ | $\text{pmol}\cdot\text{s}^{-1}\cdot 10^{-6}$ cells | $\text{amol}\cdot\text{s}^{-1}\cdot\text{cell}^{-1}$ | 2 |
| | $\text{pmol}\cdot\text{s}^{-1}\cdot 10^{-9}$ cells | $\text{zmol}\cdot\text{s}^{-1}\cdot\text{cell}^{-1}$ | 3 |
| cell number concentration, C_{Nce} | 10^6 cells $\cdot\text{mL}^{-1}$ | 10^9 cells $\cdot\text{L}^{-1}$ | |
| mitochondrial protein concentration, C_{mtE} | 0.1 mg $\cdot\text{mL}^{-1}$ | 0.1 g $\cdot\text{L}^{-1}$ | |
| mass-specific flux, $J_{O_2/m}$ | $\text{pmol}\cdot\text{s}^{-1}\cdot\text{mg}^{-1}$ | $\text{nmol}\cdot\text{s}^{-1}\cdot\text{g}^{-1}$ | 4 |
| catabolic power, P_k | $\mu\text{W}\cdot 10^{-6}$ cells | $\text{pW}\cdot\text{cell}^{-1}$ | 1 |
| volume | 1,000 L | m^3 (1,000 kg) | |
| | L | dm^3 (kg) | |
| | mL | cm^3 (g) | |
| | μL | mm^3 (mg) | |
| | fL | μm^3 (pg) | 5 |
| amount of substance concentration | $\text{M} = \text{mol}\cdot\text{L}^{-1}$ | $\text{mol}\cdot\text{dm}^{-3}$ | |

1300 1 pmol: picomole = 10^{-12} mol1301 2 amol: attomole = 10^{-18} mol1302 3 zmol: zeptomole = 10^{-21} mol

1303

1304 Although volume is expressed as m^3 using the *SI* base unit, the litre [dm^3] is a conventional unit
 1305 of volume for concentration and is used for most solution chemical kinetics. If one multiplies $I_{O_2/Nce}$ by
 1306 C_{Nce} , then the result will not only be the amount of O_2 [mol] consumed per time [s^{-1}] in one litre [L^{-1}],
 1307 but also the change in O_2 concentration per second (for any volume of an ideally closed system). This
 1308 is ideal for kinetic modeling as it blends with chemical rate equations where concentrations are typically
 1309 expressed in $\text{mol}\cdot\text{L}^{-1}$ (Wagner *et al.* 2011). In studies of multinuclear cells—such as differentiated
 1310 skeletal muscle cells—it is easy to determine the number of nuclei but not the total number of cells. A
 1311 generalized concept, therefore, is obtained by substituting cells by nuclei as the sample entity. This does
 1312 not hold, however, for enucleated platelets.

1313 For studies of cells, we recommend that respiration be expressed, as far as possible, as: (1) O_2
 1314 flux normalized for a mitochondrial marker, for separation of the effects of mitochondrial quality and
 1315 content on cell respiration (this includes *FCRs* as a normalization for a functional mitochondrial
 1316 marker); (2) O_2 flux in units of cell volume or mass, for comparison of respiration of cells with different
 1317 cell size (Renner *et al.* 2003) and with studies on tissue preparations, and (3) O_2 flow in units of attomole
 1318 (10^{-18} mol) of O_2 consumed in a second by each cell [$\text{amol}\cdot\text{s}^{-1}\cdot\text{cell}^{-1}$], numerically equivalent to
 1319 [$\text{pmol}\cdot\text{s}^{-1}\cdot 10^{-6}$ cells]. This convention allows information to be easily used when designing experiments
 1320 in which O_2 flow must be considered. For example, to estimate the volume-specific O_2 flux in an
 1321 instrument chamber that would be expected at a particular cell number concentration, one simply needs
 1322 to multiply the flow per cell by the number of cells per volume of interest. This provides the amount of
 1323 O_2 [mol] consumed per time [s^{-1}] per unit volume [L^{-1}]. At an O_2 flow of 100 $\text{amol}\cdot\text{s}^{-1}\cdot\text{cell}^{-1}$ and a cell
 1324 density of 10^9 cells $\cdot\text{L}^{-1}$ (10^6 cells $\cdot\text{mL}^{-1}$), the volume-specific O_2 flux is 100 $\text{nmol}\cdot\text{s}^{-1}\cdot\text{L}^{-1}$ (100
 1325 $\text{pmol}\cdot\text{s}^{-1}\cdot\text{mL}^{-1}$).

1326 ET-capacity in human cell types including HEK 293, primary HUVEC and fibroblasts ranges
 1327 from 50 to 180 $\text{amol}\cdot\text{s}^{-1}\cdot\text{cell}^{-1}$, measured in intact cells in the noncoupled state (see Gnaiger 2014). At
 1328 100 $\text{amol}\cdot\text{s}^{-1}\cdot\text{cell}^{-1}$ corrected for *Rox*, the current across the mt-membranes, I_{H+e} , approximates 193
 1329 $\text{pA}\cdot\text{cell}^{-1}$ or 0.2 nA per cell. See Rich (2003) for an extension of quantitative bioenergetics from the
 1330 molecular to the human scale, with a transmembrane proton flux equivalent to 520 A in an adult at a
 1331 catabolic power of -110 W. Modelling approaches illustrate the link between protonmotive force and
 1332 currents (Willis *et al.* 2016).

1333 We consider isolated mitochondria as powerhouses and proton pumps as molecular machines to
 1334 relate experimental results to energy metabolism of the intact cell. The cellular $\text{P}\gg/\text{O}_2$ based on oxidation

of glycogen is increased by the glycolytic (fermentative) substrate-level phosphorylation of 3 P_»/Glyc or 0.5 mol P_» for each mol O₂ consumed in the complete oxidation of a mol glycosyl unit (Glyc). Adding 0.5 to the mitochondrial P_»/O₂ ratio of 5.4 yields a bioenergetic cell physiological P_»/O₂ ratio close to 6. Two NADH equivalents are formed during glycolysis and transported from the cytosol into the mitochondrial matrix, either by the malate-aspartate shuttle or by the glycerophosphate shuttle (**Figure 2A**) resulting in different theoretical yields of ATP generated by mitochondria, the energetic cost of which potentially must be taken into account. Considering also substrate-level phosphorylation in the TCA cycle, this high P_»/O₂ ratio not only reflects proton translocation and OXPHOS studied in isolation, but integrates mitochondrial physiology with energy transformation in the living cell (Gnaiger 1993a).

7. Conclusions

Catabolic cell respiration is the process of exergonic and exothermic energy transformation in which scalar redox reactions are coupled to vectorial ion translocation across a semipermeable membrane, which separates the small volume of a bacterial cell or mitochondrion from the larger volume of its surroundings. The electrochemical exergy can be partially conserved in the phosphorylation of ADP to ATP or in ion pumping, or dissipated in an electrochemical short-circuit. Respiration is thus clearly distinguished from fermentation as the counterpart of cellular core energy metabolism. An O₂ flux balance scheme illustrates the relationships and general definitions (**Figures 1 and 2**).

Box 3: Recommendations for studies with mitochondrial preparations

- Normalization of respiratory rates should be provided as far as possible:
 1. *Biophysical normalization*: on a per cell basis as O₂ flow; this may not be possible when dealing with coenocytic organisms or tissues without cross-walls separating individual cells (e.g., filamentous fungi, muscle fibers)
 2. *Cellular normalization*: per g protein; per cell- or tissue-mass as mass-specific O₂ flux; per cell volume as cell volume-specific flux
 3. *Mitochondrial normalization*: per mitochondrial marker as mt-specific flux.
- With information on cell size and the use of multiple normalizations, maximum potential information is available (Renner *et al.* 2003; Wagner *et al.* 2011; Gnaiger 2014). Reporting flow in a respiratory chamber [nmol·s⁻¹] is discouraged, since it restricts the analysis to intra-experimental comparison of relative (qualitative) differences.
- Catabolic mitochondrial respiration is distinguished from residual O₂ consumption. Fluxes in mitochondrial coupling states should be, as far as possible, corrected for residual O₂ consumption.
- Different mechanisms of uncoupling should be distinguished by defined terms. The tightness of coupling relates to these uncoupling mechanisms, whereas the coupling stoichiometry varies as a function the substrate type involved in ET-pathways with either three or two redox proton pumps operating in series. Separation of tightness of coupling from the pathway-dependent coupling stoichiometry is possible only when the substrate type undergoing oxidation remains the same for respiration in LEAK-, OXPHOS-, and ET-states. In studies of the tightness of coupling, therefore, simple substrate-inhibitor combinations should be applied to exclude a shift in substrate competition which may occur when providing physiological substrate cocktails.
- In studies of isolated mitochondria, the mitochondrial recovery and yield should be reported. Experimental criteria for evaluation of purity versus integrity should be considered. Mitochondrial markers—such as citrate synthase activity as an enzymatic matrix marker—provide a link to the tissue of origin on the basis of calculating the mitochondrial recovery, *i.e.*, the fraction of mitochondrial marker obtained from a unit mass of tissue. Total mitochondrial protein is frequently applied as a mitochondrial marker, which is restricted to isolated mitochondria.
- In studies of permeabilized cells, the viability of the cell culture or cell suspension of origin should be reported. Normalization should be evaluated for total cell count or viable cell count.
- Terms and symbols are summarized in **Table 8**. Their use will facilitate transdisciplinary communication and support further developments towards a consistent theory of bioenergetics and mitochondrial physiology. Technical terms related to and defined with normal words can be used as index terms in databases, support the creation of ontologies towards semantic information processing

1391 (MitoPedia), and help in communicating analytical findings as impactful data-driven stories.
 1392 ‘Making data available without making it understandable may be worse than not making it available
 1393 at all’ (National Academies of Sciences, Engineering, and Medicine 2018). Success will depend on
 1394 taking next steps: (1) exhaustive text-mining considering Omics data and functional data; (2) network
 1395 analysis of Omics data with bioinformatics tools; (3) cross-validation with distinct bioinformatics
 1396 approaches; (4) correlation with functional data; (5) guidelines for biological validation of network
 1397 data. This is a call to carefully contribute to FAIR principles (Findable, Accessible, Interoperable,
 1398 Reusable) for the sharing of scientific data.
 1399

1400
 1401 **Table 8. Terms, symbols, and units.**
 1402

| 1403 | 1404 | 1405 | 1406 | 1407 |
|------|--------------------------------|------------------------|---|------|
| Term | Symbol | Unit | Links and comments | |
| 1407 | AOX | | Figure 2B | |
| 1408 | n_B | [mol] | | |
| 1409 | Y_{P_{\gg}/O_2} | | P \gg /O ₂ ratio measured in any respiratory state | |
| 1411 | k | | Figure 1 and 3 | |
| 1412 | J_{kO_2} | <i>varies</i> | Figure 1 and 3 | |
| 1413 | N_{ce} | [x] | $N_{ce} = N_{vce} + N_{dce}$; Table 5 | |
| 1414 | J_{rO_2} | <i>varies</i> | Figure 1 | |
| 1415 | VI | | $VI = N_{vce}/N_{ce} = 1 - N_{dce}/N_{ce}$ | |
| 1416 | z_B | | Table 6; $z_{O_2} = 4$ | |
| 1417 | CI to CIV | | respiratory ET Complexes; Figure 2B | |
| 1419 | $c_B = n_B \cdot V^{-1}$; [B] | [mol·m ⁻³] | Box 2 | |
| 1420 | CCS | | Section 2.4.1 | |
| 1421 | N_{dce} | [x] | non-viable cells, loss of plasma membrane barrier function; Table 5 | |
| 1423 | \underline{e} | [C] | Table 6 | |
| 1424 | ETS | | state; Figure 2B, Figure 4 | |
| 1425 | I_B | [mol·s ⁻¹] | system-related extensive quantity; Figure 6 | |
| 1427 | J_B | <i>varies</i> | size-specific quantity; Figure 6 | |
| 1428 | P _i | | Figure 2C | |
| 1429 | PiC | | Figure 2C | |
| 1431 | N_{vce} | [x] | viable cells, intact of plasma membrane barrier function; Table 5 | |
| 1433 | LEAK | | state; Table 1, Figure 4 | |
| 1434 | \underline{m} | [kg] | Table 4, Figure 6 | |
| 1435 | m_X | [kg] | Table 4 | |
| 1436 | m_d | [kg] | mass of sample X; Figure 6 (frequently called dry weight) | |
| 1438 | m_w | [kg] | mass of sample X; Figure 6 (frequently called wet weight) | |
| 1440 | $M_X = m_X \cdot N_X^{-1}$ | [kg·x ⁻¹] | mass of entity X; Table 4 | |
| 1441 | MITOCARTA | | https://www.broadinstitute.org/scientific-community/science/programs/metabolic-disease-program/publications/mitocarta/mitocarta-in-0 | |
| 1442 | | | | |
| 1443 | | | | |
| 1444 | | | | |
| 1445 | | | | |

| | | | | |
|------|--|--|--------------------------|---|
| 1446 | MitoPedia | | | http://www.bioblast.at/index.php/MitoPedia |
| 1447 | mitochondria or mitochondrial | mt | | Box 1 |
| 1448 | mitochondrial DNA | mtDNA | | Box 1 |
| 1449 | mitochondrial concentration | $C_{mtE} = mtE \cdot V^{-1}$ | [mtEU·m ⁻³] | Table 4 |
| 1450 | mitochondrial content | mtE_X | [mtEU·x ⁻¹] | $mtE_X = mtE \cdot N_X^{-1}$; Table 4 |
| 1451 | mitochondrial | | | |
| 1452 | elementary component | mtE | [mtEU] | quantity of mt-marker; Table 4 |
| 1453 | mitochondrial elementary unit | mtEU | <i>varies</i> | specific units for mt-marker; Table 4 |
| 1454 | mitochondrial inner membrane | mtIM | | MIM is widely used; the first M is replaced by mt; Figure 2; Box 1 |
| 1455 | | | | |
| 1456 | mitochondrial outer membrane | mtOM | | MOM is widely used; the first M is replaced by mt; Figure 2; Box 1 |
| 1457 | | | | |
| 1458 | mitochondrial recovery | Y_{mtE} | | fraction of mtE recovered in sample from the tissue of origin |
| 1459 | | | | |
| 1460 | mitochondrial yield | $Y_{mtE/m}$ | | mt-yield per tissues mass; $Y_{mtE/m} = Y_{mtE} \cdot D_{mtE}$ |
| 1461 | | | | |
| 1462 | molar format | \underline{n} | [mol] | Table 6 |
| 1463 | negative | neg | | Figure 4 |
| 1464 | number concentration of X | C_{NX} | [x·m ⁻³] | Table 4 |
| 1465 | number format | \underline{N} | [x] | Table 4, Figure 6 |
| 1466 | number of entities X | N_X | [x] | Table 4, Figure 6 |
| 1467 | number of entity B | N_B | [x] | Table 4 |
| 1468 | oxidative phosphorylation | OXPPOS | | state; Table 1, Figure 4 |
| 1469 | oxygen concentration | $c_{O_2} = n_{O_2} \cdot V^{-1}$ | [mol·m ⁻³] | [O ₂]; Section 3.2 |
| 1470 | oxygen flux, in reaction r | J_{rO_2} | <i>varies</i> | Figure 1 |
| 1471 | pathway control state | PCS | | Section 2.2 |
| 1472 | permeabilized cell number | N_{pce} | [x] | experimental permeabilization of plasma membrane; Table 5 |
| 1473 | | | | |
| 1474 | phosphorylation of ADP to ATP | P \gg | | Section 2.2 |
| 1475 | P \gg /O ₂ ratio | P \gg /O ₂ | | mechanistic $Y_{P\gg/O_2}$, calculated from pump stoichiometries; Figure 2B |
| 1476 | | | | |
| 1477 | positive | pos | | Figure 4 |
| 1478 | proton in the negative compartment | H ⁺ _{neg} | | Figure 4 |
| 1479 | proton in the positive compartment | H ⁺ _{pos} | | Figure 4 |
| 1480 | rate of electron transfer in ET state | E | | ET-capacity; Table 1 |
| 1481 | rate of LEAK respiration | L | | Table 1 |
| 1482 | rate of oxidative phosphorylation | P | | OXPPOS capacity; Table 1 |
| 1483 | rate of residual oxygen consumption | ROx | | Table 1, Figure 1 |
| 1484 | residual oxygen consumption | ROX | | state; Table 1 |
| 1485 | respiratory supercomplex | SC I _n III _n IV _n | | supramolecular assemblies composed of variable copy numbers (n) of CI, CIII and CIV; Box 1 |
| 1486 | | | | |
| 1487 | | | | |
| 1488 | specific mitochondrial density | $D_{mtE} = mtE \cdot m_X^{-1}$ | [mtEU·kg ⁻¹] | Table 4 |
| 1489 | substrate-uncoupler-inhibitor-titration protocol | SUIT | | ## |
| 1490 | | | | |
| 1491 | volume | V | [m ⁻³] | Table 7 |
| 1492 | volume format | \underline{V} | [m ⁻³] | Table 6 |
| 1493 | | | | |

1494 Experimentally, respiration is separated in mitochondrial preparations from the interactions with
 1495 the fermentative pathways of the intact cell. OXPPOS analysis is based on the study of mitochondrial
 1496 preparations complementary to bioenergetic investigations of intact cells and organisms—from model
 1497 organisms to the human species including healthy and diseased persons (patients). Different mechanisms
 1498 of respiratory uncoupling have to be distinguished (**Figure 3**). Metabolic fluxes measured in defined
 1499 coupling and pathway control states (**Figures 5 and 6**) provide insights into the meaning of cellular and
 1500 organismic respiration.

1501 The optimal choice for expressing mitochondrial and cell respiration as O₂ flow per biological
 1502 sample, and normalization for specific tissue-markers (volume, mass, protein) and mitochondrial
 1503 markers (volume, protein, content, mtDNA, activity of marker enzymes, respiratory reference state) is
 1504 guided by the scientific question under study. Interpretation of the data depends critically on appropriate
 1505 normalization (**Figure 6**).

1506 MitoEAGLE can serve as a gateway to better diagnose mitochondrial respiratory adaptations and
 1507 defects linked to genetic variation, age-related health risks, sex-specific mitochondrial performance,
 1508 lifestyle with its effects on degenerative diseases, and thermal and chemical environment. The present
 1509 recommendations on coupling control states and rates, linked to the concept of the protonmotive force,
 1510 are focused on studies with mitochondrial preparations (**Box 3**). These will be extended in a series of
 1511 reports on pathway control of mitochondrial respiration, respiratory states in intact cells, and
 1512 harmonization of experimental procedures.

1514 Acknowledgements

1515 We thank M. Beno for management assistance. This publication is based upon work from COST Action
 1516 CA15203 MitoEAGLE, supported by COST (European Cooperation in Science and Technology), and
 1517 K-Regio project MitoFit (E.G.).

1519 **Competing financial interests:** E.G. is founder and CEO of Oroboros Instruments, Innsbruck, Austria.

1521 References

- 1522 Altmann R (1894) Die Elementarorganismen und ihre Beziehungen zu den Zellen. Zweite vermehrte Auflage.
 1523 Verlag Von Veit & Comp, Leipzig:160 pp.
- 1525 Baggeto LG, Testa-Perussini R (1990) Role of acetoin on the regulation of intermediate metabolism of Ehrlich
 1526 ascites tumor mitochondria: its contribution to membrane cholesterol enrichment modifying passive proton
 1527 permeability. Arch Biochem Biophys 283:341-8.
- 1528 Beard DA (2005) A biophysical model of the mitochondrial respiratory system and oxidative phosphorylation.
 1529 PLoS Comput Biol 1(4):e36.
- 1530 Benda C (1898) Weitere Mitteilungen über die Mitochondria. Verh Dtsch Physiol Ges:376-83.
- 1531 Birkedal R, Laasmaa M, Vendelin M (2014) The location of energetic compartments affects energetic
 1532 communication in cardiomyocytes. Front Physiol 5:376.
- 1533 Blier PU, Dufresne F, Burton RS (2001) Natural selection and the evolution of mtDNA-encoded peptides:
 1534 evidence for intergenomic co-adaptation. Trends Genet 17:400-6.
- 1535 Blier PU, Guderley HE (1993) Mitochondrial activity in rainbow trout red muscle: the effect of temperature on
 1536 the ADP-dependence of ATP synthesis. J Exp Biol 176:145-58.
- 1537 Breton S, Beaupré HD, Stewart DT, Hoeh WR, Blier PU (2007) The unusual system of doubly uniparental
 1538 inheritance of mtDNA: isn't one enough? Trends Genet 23:465-74.
- 1539 Brown GC (1992) Control of respiration and ATP synthesis in mammalian mitochondria and cells. Biochem J
 1540 284:1-13.
- 1541 Burger G, Gray MW, Forget L, Lang BF (2013) Strikingly bacteria-like and gene-rich mitochondrial genomes
 1542 throughout jakobid protists. Genome Biol Evol 5:418-38.
- 1543 Calvo SE, Klauser CR, Mootha VK (2016) MitoCarta2.0: an updated inventory of mammalian mitochondrial
 1544 proteins. Nucleic Acids Research 44:D1251-7.
- 1545 Calvo SE, Julien O, Clauser KR, Shen H, Kamer KJ, Wells JA, Mootha VK (2017) Comparative analysis of
 1546 mitochondrial N-termini from mouse, human, and yeast. Mol Cell Proteomics 16:512-23.
- 1547 Campos JC, Queliconi BB, Bozi LHM, Bechara LRG, Dourado PMM, Andres AM, Jannig PR, Gomes KMS,
 1548 Zambelli VO, Rocha-Resende C, Guatimosim S, Brum PC, Mochly-Rosen D, Gottlieb RA, Kowaltowski AJ,
 1549 Ferreira JCB (2017) Exercise reestablishes autophagic flux and mitochondrial quality control in heart failure.
 1550 Autophagy 13:1304-317.
- 1551 Canton M, Luvisetto S, Schmehl I, Azzone GF (1995) The nature of mitochondrial respiration and
 1552 discrimination between membrane and pump properties. Biochem J 310:477-81.
- 1553 Carrico C, Meyer JG, He W, Gibson BW, Verdin E (2018) The mitochondrial acylome emerges: proteomics,
 1554 regulation by Sirtuins, and metabolic and disease implications. Cell Metab 27:497-512.
- 1555 Chan DC (2006) Mitochondria: dynamic organelles in disease, aging, and development. Cell 125:1241-52.
- 1556 Chance B, Williams GR (1955a) Respiratory enzymes in oxidative phosphorylation. I. Kinetics of oxygen
 1557 utilization. J Biol Chem 217:383-93.
- 1558 Chance B, Williams GR (1955b) Respiratory enzymes in oxidative phosphorylation: III. The steady state. J Biol
 1559 Chem 217:409-27.

- 1560 Chance B, Williams GR (1955c) Respiratory enzymes in oxidative phosphorylation. IV. The respiratory chain. J
 1561 Biol Chem 217:429-38.
- 1562 Chance B, Williams GR (1956) The respiratory chain and oxidative phosphorylation. Adv Enzymol Relat Subj
 1563 Biochem 17:65-134.
- 1564 Chowdhury SK, Djordjevic J, Albensi B, Fernyhough P (2015) Simultaneous evaluation of substrate-dependent
 1565 oxygen consumption rates and mitochondrial membrane potential by TMRM and safranin in cortical
 1566 mitochondria. Biosci Rep 36:e00286.
- 1567 Cobb LJ, Lee C, Xiao J, Yen K, Wong RG, Nakamura HK, Mehta HH, Gao Q, Ashur C, Huffman DM, Wan J,
 1568 Muzumdar R, Barzilai N, Cohen P (2016) Naturally occurring mitochondrial-derived peptides are age-
 1569 dependent regulators of apoptosis, insulin sensitivity, and inflammatory markers. Aging (Albany NY) 8:796-
 1570 809.
- 1571 Cohen ER, Cvitas T, Frey JG, Holmström B, Kuchitsu K, Marquardt R, Mills I, Pavese F, Quack M, Stohner J,
 1572 Strauss HL, Takami M, Thor HL (2008) Quantities, units and symbols in physical chemistry, IUPAC Green
 1573 Book, 3rd Edition, 2nd Printing, IUPAC & RSC Publishing, Cambridge.
- 1574 Cooper H, Hedges LV, Valentine JC, eds (2009) The handbook of research synthesis and meta-analysis. Russell
 1575 Sage Foundation.
- 1576 Coopersmith J (2010) Energy, the subtle concept. The discovery of Feynman's blocks from Leibnitz to Einstein.
 1577 Oxford University Press:400 pp.
- 1578 Cummins J (1998) Mitochondrial DNA in mammalian reproduction. Rev Reprod 3:172-82.
- 1579 Dai Q, Shah AA, Garde RV, Yonish BA, Zhang L, Medvitz NA, Miller SE, Hansen EL, Dunn CN, Price TM
 1580 (2013) A truncated progesterone receptor (PR-M) localizes to the mitochondrion and controls cellular
 1581 respiration. Mol Endocrinol 27:741-53.
- 1582 Daum B, Walter A, Horst A, Osiewacz HD, Kühlbrandt W (2013) Age-dependent dissociation of ATP synthase
 1583 dimers and loss of inner-membrane cristae in mitochondria. Proc Natl Acad Sci U S A 110:15301-6.
- 1584 Divakaruni AS, Brand MD (2011) The regulation and physiology of mitochondrial proton leak. Physiology
 1585 (Bethesda) 26:192-205.
- 1586 Doerrier C, Garcia-Souza LF, Krumschnabel G, Wohlfarter Y, Mészáros AT, Gnaiger E (2018) High-Resolution
 1587 FluoRespirometry and OXPHOS protocols for human cells, permeabilized fibres from small biopsies of
 1588 muscle, and isolated mitochondria. Methods Mol Biol 1782 (Palmeira CM, Moreno AJ, eds): Mitochondrial
 1589 Bioenergetics, 978-1-4939-7830-4.
- 1590 Doskey CM, van 't Erve TJ, Wagner BA, Buettner GR (2015) Moles of a substance per cell is a highly
 1591 informative dosing metric in cell culture. PLOS ONE 10:e0132572.
- 1592 Drahota Z, Milerová M, Stieglerová A, Houstek J, Ostádal B (2004) Developmental changes of cytochrome c
 1593 oxidase and citrate synthase in rat heart homogenate. Physiol Res 53:119-22.
- 1594 Duarte FV, Palmeira CM, Rolo AP (2014) The role of microRNAs in mitochondria: small players acting wide.
 1595 Genes (Basel) 5:865-86.
- 1596 Ehinger JK, Morota S, Hansson MJ, Paul G, Elmér E (2015) Mitochondrial dysfunction in blood cells from
 1597 amyotrophic lateral sclerosis patients. J Neurol 262:1493-503.
- 1598 Ernster L, Schatz G (1981) Mitochondria: a historical review. J Cell Biol 91:227s-55s.
- 1599 Estabrook RW (1967) Mitochondrial respiratory control and the polarographic measurement of ADP:O ratios.
 1600 Methods Enzymol 10:41-7.
- 1601 Faber C, Zhu ZJ, Castellino S, Wagner DS, Brown RH, Peterson RA, Gates L, Barton J, Bickett M, Hagerty L,
 1602 Kimbrough C, Sola M, Bailey D, Jordan H, Elangbam CS (2014) Cardiolipin profiles as a potential
 1603 biomarker of mitochondrial health in diet-induced obese mice subjected to exercise, diet-restriction and
 1604 ephedrine treatment. J Appl Toxicol 34:1122-9.
- 1605 Feagin JE, Harrell MI, Lee JC, Coe KJ, Sands BH, Cannone JJ, Tami G, Schnare MN, Gutell RR (2012) The
 1606 fragmented mitochondrial ribosomal RNAs of *Plasmodium falciparum*. PLoS One 7:e38320.
- 1607 Fell D (1997) Understanding the control of metabolism. Portland Press.
- 1608 Forstner H, Gnaiger E (1983) Calculation of equilibrium oxygen concentration. In: Polarographic Oxygen
 1609 Sensors. Aquatic and Physiological Applications. Gnaiger E, Forstner H (eds), Springer, Berlin, Heidelberg,
 1610 New York:321-33.
- 1611 Garlid KD, Beavis AD, Ratkje SK (1989) On the nature of ion leaks in energy-transducing membranes. Biochim
 1612 Biophys Acta 976:109-20.
- 1613 Garlid KD, Semrad C, Zinchenko V. Does redox slip contribute significantly to mitochondrial respiration? In:
 1614 Schuster S, Rigoulet M, Ouhabi R, Mazat J-P, eds (1993) Modern trends in biothermokinetics. Plenum Press,
 1615 New York, London:287-93.
- 1616 Gerö D, Szabo C (2016) Glucocorticoids suppress mitochondrial oxidant production via upregulation of
 1617 uncoupling protein 2 in hyperglycemic endothelial cells. PLoS One 11:e0154813.
- 1618 Gnaiger E. Efficiency and power strategies under hypoxia. Is low efficiency at high glycolytic ATP production a
 1619 paradox? In: Surviving Hypoxia: Mechanisms of Control and Adaptation. Hochachka PW, Lutz PL, Sick T,
 1620 Rosenthal M, Van den Thillart G, eds (1993a) CRC Press, Boca Raton, Ann Arbor, London, Tokyo:77-109.
- 1621 Gnaiger E (1993b) Nonequilibrium thermodynamics of energy transformations. Pure Appl Chem 65:1983-2002.

- 1622 Gnaiger E (2001) Bioenergetics at low oxygen: dependence of respiration and phosphorylation on oxygen and
 1623 adenosine diphosphate supply. *Respir Physiol* 128:277-97.
- 1624 Gnaiger E (2009) Capacity of oxidative phosphorylation in human skeletal muscle. New perspectives of
 1625 mitochondrial physiology. *Int J Biochem Cell Biol* 41:1837-45.
- 1626 Gnaiger E (2014) Mitochondrial pathways and respiratory control. An introduction to OXPHOS analysis. 4th ed.
 1627 Mitochondr Physiol Network 19.12. Oroboros MiPNet Publications, Innsbruck:80 pp.
- 1628 Gnaiger E, Méndez G, Hand SC (2000) High phosphorylation efficiency and depression of uncoupled respiration
 1629 in mitochondria under hypoxia. *Proc Natl Acad Sci USA* 97:11080-5.
- 1630 Greggio C, Jha P, Kulkarni SS, Lagarrigue S, Broskey NT, Boutant M, Wang X, Conde Alonso S, Ofori E,
 1631 Auwerx J, Cantó C, Amati F (2017) Enhanced respiratory chain supercomplex formation in response to
 1632 exercise in human skeletal muscle. *Cell Metab* 25:301-11.
- 1633 Hinkle PC (2005) P/O ratios of mitochondrial oxidative phosphorylation. *Biochim Biophys Acta* 1706:1-11.
- 1634 Hofstadter DR (1979) Gödel, Escher, Bach: An eternal golden braid. A metaphorical fugue on minds and
 1635 machines in the spirit of Lewis Carroll. Harvester Press:499 pp.
- 1636 Illaste A, Laasmaa M, Peterson P, Vendelin M (2012) Analysis of molecular movement reveals latticelike
 1637 obstructions to diffusion in heart muscle cells. *Biophys J* 102:739-48.
- 1638 Jasienski M, Bazzaz FA (1999) The fallacy of ratios and the testability of models in biology. *Oikos* 84:321-26.
- 1639 Jepihhina N, Beraud N, Sepp M, Birkedal R, Vendelin M (2011) Permeabilized rat cardiomyocyte response
 1640 demonstrates intracellular origin of diffusion obstacles. *Biophys J* 101:2112-21.
- 1641 Karnkowska A, Vacek V, Zubáčová Z, Treitli SC, Petrželková R, Eme L, Novák L, Žárský V, Barlow LD,
 1642 Herman EK, Soukal P, Hroudová M, Doležal P, Stairs CW, Roger AJ, Eliáš M, Dacks JB, Vlček Č, Hampl V
 1643 (2016) A eukaryote without a mitochondrial organelle. *Curr Biol* 26:1274-84.
- 1644 Klepinin A, Ounpuu L, Guzun R, Chekulayev V, Timohhina N, Tepp K, Shevchuk I, Schlattner U, Kaambre T
 1645 (2016) Simple oxygraphic analysis for the presence of adenylate kinase 1 and 2 in normal and tumor cells. *J*
 1646 *Bioenerg Biomembr* 48:531-48.
- 1647 Klingenberg M (2017) UCP1 - A sophisticated energy valve. *Biochimie* 134:19-27.
- 1648 Koit A, Shevchuk I, Ounpuu L, Klepinin A, Chekulayev V, Timohhina N, Tepp K, Puurand M, Truu L, Heck K,
 1649 Valvere V, Guzun R, Kaambre T (2017) Mitochondrial respiration in human colorectal and breast cancer
 1650 clinical material is regulated differently. *Oxid Med Cell Longev* 1372640.
- 1651 Komlódi T, Tretter L (2017) Methylene blue stimulates substrate-level phosphorylation catalysed by succinyl-
 1652 CoA ligase in the citric acid cycle. *Neuropharmacology* 123:287-98.
- 1653 Korn E (1969) Cell membranes: structure and synthesis. *Annu Rev Biochem* 38:263-88.
- 1654 Lai N, M Kummitha C, Rosca MG, Fujioka H, Tandler B, Hoppel CL (2018) Isolation of mitochondrial
 1655 subpopulations from skeletal muscle: optimizing recovery and preserving integrity. *Acta Physiol*
 1656 (Oxf):e13182. doi: 10.1111/apha.13182.
- 1657 Lane N (2005) Power, sex, suicide: mitochondria and the meaning of life. Oxford University Press:354 pp.
- 1658 Larsen S, Nielsen J, Neigaard Nielsen C, Nielsen LB, Wibrand F, Stride N, Schroder HD, Boushel RC, Helge
 1659 JW, Dela F, Hey-Mogensen M (2012) Biomarkers of mitochondrial content in skeletal muscle of healthy
 1660 young human subjects. *J Physiol* 590:3349-60.
- 1661 Lee C, Zeng J, Drew BG, Sallam T, Martin-Montalvo A, Wan J, Kim SJ, Mehta H, Hevener AL, de Cabo R,
 1662 Cohen P (2015) The mitochondrial-derived peptide MOTS-c promotes metabolic homeostasis and reduces
 1663 obesity and insulin resistance. *Cell Metab* 21:443-54.
- 1664 Lee SR, Kim HK, Song IS, Youm J, Dizon LA, Jeong SH, Ko TH, Heo HJ, Ko KS, Rhee BD, Kim N, Han J
 1665 (2013) Glucocorticoids and their receptors: insights into specific roles in mitochondria. *Prog Biophys Mol*
 1666 *Biol* 112:44-54.
- 1667 Leek BT, Mudaliar SR, Henry R, Mathieu-Costello O, Richardson RS (2001) Effect of acute exercise on citrate
 1668 synthase activity in untrained and trained human skeletal muscle. *Am J Physiol Regul Integr Comp Physiol*
 1669 280:R441-7.
- 1670 Lemieux H, Blier PU, Gnaiger E (2017) Remodeling pathway control of mitochondrial respiratory capacity by
 1671 temperature in mouse heart: electron flow through the Q-junction in permeabilized fibers. *Sci Rep* 7:2840.
- 1672 Lenaz G, Tioli G, Falasca AI, Genova ML (2017) Respiratory supercomplexes in mitochondria. In: Mechanisms
 1673 of primary energy trasduction in biology. M Wikstrom (ed) Royal Society of Chemistry Publishing, London,
 1674 UK:296-337.
- 1675 Liu S, Roellig DM, Guo Y, Li N, Frace MA, Tang K, Zhang L, Feng Y, Xiao L (2016) Evolution of mitosome
 1676 metabolism and invasion-related proteins in *Cryptosporidium*. *BMC Genomics* 17:1006.
- 1677 Margulis L (1970) Origin of eukaryotic cells. New Haven: Yale University Press.
- 1678 Meinild Lundby AK, Jacobs RA, Gehrig S, de Leur J, Hauser M, Bonne TC, Flück D, Dandanell S, Kirk N,
 1679 Kaech A, Ziegler U, Larsen S, Lundby C (2018) Exercise training increases skeletal muscle mitochondrial
 1680 volume density by enlargement of existing mitochondria and not de novo biogenesis. *Acta Physiol* 222,
 1681 e12905.

- 1682 Menshikova EV, Ritov VB, Fairfull L, Ferrell RE, Kelley DE, Goodpaster BH (2006) Effects of exercise on
1683 mitochondrial content and function in aging human skeletal muscle. *J Gerontol A Biol Sci Med Sci* 61:534-
1684 40.
- 1685 Menshikova EV, Ritov VB, Ferrell RE, Azuma K, Goodpaster BH, Kelley DE (2007) Characteristics of skeletal
1686 muscle mitochondrial biogenesis induced by moderate-intensity exercise and weight loss in obesity. *J Appl*
1687 *Physiol* (1985) 103:21-7.
- 1688 Menshikova EV, Ritov VB, Toledo FG, Ferrell RE, Goodpaster BH, Kelley DE (2005) Effects of weight loss
1689 and physical activity on skeletal muscle mitochondrial function in obesity. *Am J Physiol Endocrinol Metab*
1690 288:E818-25.
- 1691 Miller GA (1991) *The science of words*. Scientific American Library New York:276 pp.
- 1692 Mitchell P (1961) Coupling of phosphorylation to electron and hydrogen transfer by a chemi-osmotic type of
1693 mechanism. *Nature* 191:144-8.
- 1694 Mitchell P (2011) Chemiosmotic coupling in oxidative and photosynthetic phosphorylation. *Biochim Biophys*
1695 *Acta Bioenergetics* 1807:1507-38.
- 1696 Mogensen M, Sahlin K, Fernström M, Glintborg D, Vind BF, Beck-Nielsen H, Højlund K (2007) Mitochondrial
1697 respiration is decreased in skeletal muscle of patients with type 2 diabetes. *Diabetes* 56:1592-9.
- 1698 Mohr PJ, Phillips WD (2015) Dimensionless units in the SI. *Metrologia* 52:40-7.
- 1699 Moreno M, Giacco A, Di Munno C, Goglia F (2017) Direct and rapid effects of 3,5-diiodo-L-thyronine (T2).
1700 *Mol Cell Endocrinol* 7207:30092-8.
- 1701 Morrow RM, Picard M, Derbeneva O, Leipzig J, McManus MJ, Gousspillou G, Barbat-Artigas S, Dos Santos C,
1702 Hepple RT, Murdock DG, Wallace DC (2017) Mitochondrial energy deficiency leads to hyperproliferation of
1703 skeletal muscle mitochondria and enhanced insulin sensitivity. *Proc Natl Acad Sci U S A* 114:2705-10.
- 1704 Murley A, Nunnari J (2016) The emerging network of mitochondria-organelle contacts. *Mol Cell* 61:648-53.
- 1705 National Academies of Sciences, Engineering, and Medicine (2018) International coordination for science data
1706 infrastructure: Proceedings of a workshop—in brief. Washington, DC: The National Academies Press. doi:
1707 <https://doi.org/10.17226/25015>.
- 1708 Oemer G, Lackner L, Muigg K, Krumschnabel G, Watschinger K, Sailer S, Lindner H, Gnaiger E, Wortmann
1709 SB, Werner ER, Zschocke J, Keller MA (2018) The molecular structural diversity of mitochondrial
1710 cardiolipins. *Proc Nat Acad Sci U S A* 115:4158-63.
- 1711 Palmfeldt J, Bross P (2017) Proteomics of human mitochondria. *Mitochondrion* 33:2-14.
- 1712 Paradies G, Paradies V, De Benedictis V, Ruggiero FM, Petrosillo G (2014) Functional role of cardiolipin in
1713 mitochondrial bioenergetics. *Biochim Biophys Acta* 1837:408-17.
- 1714 Pesta D, Gnaiger E (2012) High-Resolution Respirometry. OXPHOS protocols for human cells and
1715 permeabilized fibres from small biopsies of human muscle. *Methods Mol Biol* 810:25-58.
- 1716 Pesta D, Hoppel F, Macek C, Messner H, Faulhaber M, Kobel C, Parson W, Burtscher M, Schocke M, Gnaiger
1717 E (2011) Similar qualitative and quantitative changes of mitochondrial respiration following strength and
1718 endurance training in normoxia and hypoxia in sedentary humans. *Am J Physiol Regul Integr Comp Physiol*
1719 301:R1078-87.
- 1720 Price TM, Dai Q (2015) The role of a mitochondrial progesterone receptor (PR-M) in progesterone action.
1721 *Semin Reprod Med* 33:185-94.
- 1722 Puchowicz MA, Varnes ME, Cohen BH, Friedman NR, Kerr DS, Hoppel CL (2004) Oxidative phosphorylation
1723 analysis: assessing the integrated functional activity of human skeletal muscle mitochondria – case studies.
1724 *Mitochondrion* 4:377-85. Puntchart A, Claassen H, Jostarndt K, Hoppeler H, Billeter R (1995) mRNAs of
1725 enzymes involved in energy metabolism and mtDNA are increased in endurance-trained athletes. *Am J*
1726 *Physiol* 269:C619-25.
- 1727 Quiros PM, Mottis A, Auwerx J (2016) Mitonuclear communication in homeostasis and stress. *Nat Rev Mol*
1728 *Cell Biol* 17:213-26.
- 1729 Rackham O, Mercer TR, Filipovska A (2012) The human mitochondrial transcriptome and the RNA-binding
1730 proteins that regulate its expression. *WIREs RNA* 3:675-95.
- 1731 Reichmann H, Hoppeler H, Mathieu-Costello O, von Bergen F, Pette D (1985) Biochemical and ultrastructural
1732 changes of skeletal muscle mitochondria after chronic electrical stimulation in rabbits. *Pflügers Arch* 404:1-
1733 9.
- 1734 Renner K, Amberger A, Konwalinka G, Gnaiger E (2003) Changes of mitochondrial respiration, mitochondrial
1735 content and cell size after induction of apoptosis in leukemia cells. *Biochim Biophys Acta* 1642:115-23.
- 1736 Rice DW, Alverson AJ, Richardson AO, Young GJ, Sanchez-Puerta MV, Munzinger J, Barry K, Boore JL,
1737 Zhang Y, dePamphilis CW, Knox EB, Palmer JD (2016) Horizontal transfer of entire genomes via
1738 mitochondrial fusion in the angiosperm *Amborella*. *Science* 342:1468-73.
- 1739 Rich P (2003) Chemiosmotic coupling: The cost of living. *Nature* 421:583.
- 1740 Rich PR (2013) Chemiosmotic theory. *Encyclopedia Biol Chem* 1:467-72.
- 1741 Roger JA, Munoz-Gomes SA, Kamikawa R (2017) The origin and diversification of mitochondria. *Curr Biol*
1742 27:R1177-92.

- 1743 Rostovtseva TK, Sheldon KL, Hassanzadeh E, Monge C, Saks V, Bezrukov SM, Sackett DL (2008) Tubulin
1744 binding blocks mitochondrial voltage-dependent anion channel and regulates respiration. *Proc Natl Acad Sci*
1745 *USA* 105:18746-51.
- 1746 Rustin P, Parfait B, Chretien D, Bourgeron T, Djouadi F, Bastin J, Rötig A, Munnich A (1996) Fluxes of
1747 nicotinamide adenine dinucleotides through mitochondrial membranes in human cultured cells. *J Biol Chem*
1748 271:14785-90.
- 1749 Saks VA, Veksler VI, Kuznetsov AV, Kay L, Sikk P, Tiivel T, Tranqui L, Olivares J, Winkler K, Wiedemann F,
1750 Kunz WS (1998) Permeabilised cell and skinned fiber techniques in studies of mitochondrial function in
1751 vivo. *Mol Cell Biochem* 184:81-100.
- 1752 Salabei JK, Gibb AA, Hill BG (2014) Comprehensive measurement of respiratory activity in permeabilized cells
1753 using extracellular flux analysis. *Nat Protoc* 9:421-38.
- 1754 Sazanov LA (2015) A giant molecular proton pump: structure and mechanism of respiratory complex I. *Nat Rev*
1755 *Mol Cell Biol* 16:375-88.
- 1756 Schneider TD (2006) Claude Shannon: biologist. The founder of information theory used biology to formulate
1757 the channel capacity. *IEEE Eng Med Biol Mag* 25:30-3.
- 1758 Schönfeld P, Dymkowska D, Wojtczak L (2009) Acyl-CoA-induced generation of reactive oxygen species in
1759 mitochondrial preparations is due to the presence of peroxisomes. *Free Radic Biol Med* 47:503-9.
- 1760 Schultz J, Wiesner RJ (2000) Proliferation of mitochondria in chronically stimulated rabbit skeletal muscle--
1761 transcription of mitochondrial genes and copy number of mitochondrial DNA. *J Bioenerg Biomembr* 32:627-
1762 34.
- 1763 Speijer D (2016) Being right on Q: shaping eukaryotic evolution. *Biochem J* 473:4103-27.
- 1764 Sugiura A, Mattie S, Prudent J, McBride HM (2017) Newly born peroxisomes are a hybrid of mitochondrial and
1765 ER-derived pre-peroxisomes. *Nature* 542:251-4.
- 1766 Simson P, Jepihhina N, Laasmaa M, Peterson P, Birkedal R, Vendelin M (2016) Restricted ADP movement in
1767 cardiomyocytes: Cytosolic diffusion obstacles are complemented with a small number of open mitochondrial
1768 voltage-dependent anion channels. *J Mol Cell Cardiol* 97:197-203.
- 1769 Stucki JW, Ineichen EA (1974) Energy dissipation by calcium recycling and the efficiency of calcium transport
1770 in rat-liver mitochondria. *Eur J Biochem* 48:365-75.
- 1771 Tonkonogi M, Harris B, Sahlin K (1997) Increased activity of citrate synthase in human skeletal muscle after a
1772 single bout of prolonged exercise. *Acta Physiol Scand* 161:435-6.
- 1773 Torralba D, Baixauli F, Sánchez-Madrid F (2016) Mitochondria know no boundaries: mechanisms and functions
1774 of intercellular mitochondrial transfer. *Front Cell Dev Biol* 4:107. eCollection 2016.
- 1775 Vamecq J, Schepers L, Parmentier G, Mannaerts GP (1987) Inhibition of peroxisomal fatty acyl-CoA oxidase by
1776 antimycin A. *Biochem J* 248:603-7.
- 1777 Waczulikova I, Habodaszova D, Cagalinec M, Ferko M, Ulicna O, Mateasik A, Sikurova L, Ziegelhöffer A
1778 (2007) Mitochondrial membrane fluidity, potential, and calcium transients in the myocardium from acute
1779 diabetic rats. *Can J Physiol Pharmacol* 85:372-81.
- 1780 Wagner BA, Venkataraman S, Buettner GR (2011) The rate of oxygen utilization by cells. *Free Radic Biol Med*
1781 51:700-712.
- 1782 Wang H, Hiatt WR, Barstow TJ, Brass EP (1999) Relationships between muscle mitochondrial DNA content,
1783 mitochondrial enzyme activity and oxidative capacity in man: alterations with disease. *Eur J Appl Physiol*
1784 *Occup Physiol* 80:22-7.
- 1785 Watt IN, Montgomery MG, Runswick MJ, Leslie AG, Walker JE (2010) Bioenergetic cost of making an
1786 adenosine triphosphate molecule in animal mitochondria. *Proc Natl Acad Sci U S A* 107:16823-7.
- 1787 Weibel ER, Hoppeler H (2005) Exercise-induced maximal metabolic rate scales with muscle aerobic capacity. *J*
1788 *Exp Biol* 208:1635-44.
- 1789 White DJ, Wolff JN, Pierson M, Gemmell NJ (2008) Revealing the hidden complexities of mtDNA inheritance.
1790 *Mol Ecol* 17:4925-42.
- 1791 Wikström M, Hummer G (2012) Stoichiometry of proton translocation by respiratory complex I and its
1792 mechanistic implications. *Proc Natl Acad Sci U S A* 109:4431-6.
- 1793 Williams EG, Wu Y, Jha P, Dubuis S, Blattmann P, Argmann CA, Houten SM, Amariuta T, Wolski W,
1794 Zamboni N, Aebersold R, Auwerx J (2016) Systems proteomics of liver mitochondria function. *Science* 352
1795 (6291):aad0189
- 1796 Willis WT, Jackman MR, Messer JI, Kuzmiak-Glancy S, Glancy B (2016) A simple hydraulic analog model of
1797 oxidative phosphorylation. *Med Sci Sports Exerc* 48:990-1000.
- 1798 Zíková A, Hampl V, Paris Z, Týč J, Lukeš J (2016) Aerobic mitochondria of parasitic protists: diverse genomes
1799 and complex functions. *Mol Biochem Parasitol* 209:46-57.
- 1800
- 1801

1802 **Supplement**
1803

1804 **S1. Manuscript phases and versions - an open-access approach**
1805

1806 This manuscript on ‘Mitochondrial respiratory states and rates’ is a position statement in the frame of COST Action
1807 CA15203 MitoEAGLE. The list of co-authors evolved beyond phase 1 in the bottom-up spirit of COST.

1808 The global MitoEAGLE network made it possible to collaborate with a large number of co-authors to reach
1809 consensus on the present manuscript. Nevertheless, we do not consider scientific progress to be supported by
1810 ‘declaration’ statements (other than on ethical or political issues). Our manuscript aims at providing arguments for
1811 further debate rather than pushing opinions. We hope to initiate a much broader process of discussion and want to
1812 raise the awareness on the importance of a consistent terminology for reporting of scientific data in the field of
1813 bioenergetics, mitochondrial physiology and pathology. Quality of research requires quality of communication.
1814 Some established researchers in the field may not want to re-consider the use of jargon which has become
1815 established despite deficiencies of accuracy and meaning. In the long run, superior standards will become accepted.
1816 We hope to contribute to this evolutionary process, with an emphasis on harmonization rather than standardization.

1817 *Phase 1* The protonmotive force and respiratory control

1818 http://www.mitoeagle.org/index.php/The_protonmotive_force_and_respiratory_control

1819 • 2017-04-09 to 2017-09-18 (44 versions)

1820 • 2017-09-21 to 2018-02-06 (21 versions)

1821 http://www.mitoeagle.org/index.php/MitoEAGLE_preprint_2017-09-21

1822 2017-11-11: Print version (16) for MiP2017/MitoEAGLE conference in Hradec Kralove

1823 *Phase 2* Mitochondrial respiratory states and rates: Building blocks of mitochondrial physiology Part 1

1824 http://www.mitoeagle.org/index.php/MitoEAGLE_preprint_2018-02-08

1825 • 2018-02-08 – (42 Versions up to 2018-09-24)

1826 *Phase 3* Submission to a preprint server: [BioRxiv](https://www.biorxiv.org/)

1827 *Phase 4* Journal submission

1828 CELL METABOLISM, aiming at indexing by *The Web of Science* and *PubMed*. We expect feedback from
1829 many colleagues until the end of May, to prepare a final circular to all co-authors in June 2018.
1830
1831

1832 **S2. Authors**
1833

1834 This manuscript developed as an open invitation to scientists and students to join as co-authors, to provide a
1835 balanced view on mitochondrial respiratory control and a consensus statement on reporting data of mitochondrial
1836 respiration in terms of metabolic flows and fluxes.

1837 Co-authors are added in alphabetical order based upon a first draft written by the corresponding author, who
1838 edited all versions. *Co-authors confirm to have read the final manuscript, possibly have made additions or*
1839 *suggestions for improvement, and agree to implement the recommendations into future manuscripts, presentations*
1840 *and teaching materials.*

1841 We continue to invite comments and suggestions, particularly if you are an early career investigator adding
1842 an open future-oriented perspective, or an established scientist providing a balanced historical basis. Your critical
1843 input into the quality of the manuscript will be most welcome, improving our aims to be educational, general,
1844 consensus-oriented, and practically helpful for students working in mitochondrial respiratory physiology.

1845 To join as a co-author, please feel free to focus on a particular section, providing direct input and references,
1846 and contributing to the scope of the manuscript from the perspective of your expertise. Your comments will be
1847 largely posted on the discussion page of the MitoEAGLE preprint website.

1848 If you prefer to submit comments in the format of a referee's evaluation rather than a contribution as a co-
1849 author, we will be glad to distribute your views to the updated list of co-authors for a balanced response. We would
1850 ask for your consent on this open bottom-up policy.
1851
1852

1853 **S3. Joining COST Actions**
1854

1855 • CA15203 MitoEAGLE - http://www.cost.eu/COST_Actions/ca/CA15203

1856 • CA16225 EU-CARDIOPROTECTION - http://www.cost.eu/COST_Actions/ca/CA16225

1857 • CA17129 CardioRNA - http://www.cost.eu/COST_Actions/ca/CA17129



Mitochondrial respiratory states and rates:



Building blocks of mitochondrial physiology

Part 1 - www.mitoeagle.org/index.php/MitoEAGLE_preprint_2018-02-08

Gnaiger E^{1,2}, corresponding author
355 co-authors, MitoEAGLE Working Group

¹Medical University Innsbruck
²Oroboros, Innsbruck, Austria

Aims Clarity of concept and consistency of nomenclature facilitate effective transdisciplinary communication, education, and ultimately further discovery.

Adhering to uniform standards and harmonizing the terminology concerning mitochondrial respiratory states and rates will support the development of databases of mitochondrial respiratory function in cells, tissues, and species.

Summary Recommendations on coupling control states and rates are focused on studies with mitochondrial preparations.

Fig. 1: Respiration is defined by O₂ flux balance.

Fig. 2: OXPHOS analysis is based on the study of mt- preparations. Metabolic fluxes measured in defined coupling and pathway control states provide insights into the meaning of cellular respiration.

Fig. 3: Interpretation of respiratory rates depends critically on appropriate normalization.

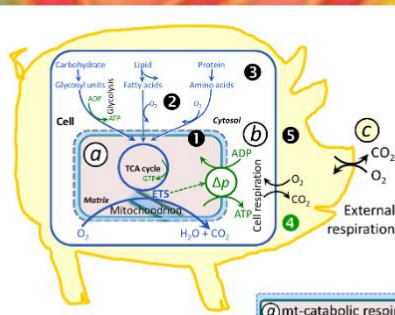
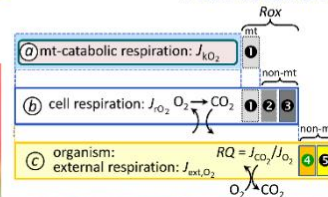


Figure 1. From mitochondrial to external respiration

Mitochondrial (mt) respiration is the oxidation of fuel substrates (electron donors) and reduction of O₂ catalysed by the electron transfer system, ETS:

- a** mt-catabolic respiration, excluding
- 1** mt-residual oxygen consumption, *Rox*.
- b** Total cellular O₂ consumption, including mt-*Rox*,
- e** non-mt catabolic *Rox*, particularly by peroxisomal oxidases, and
- 9** non-mt *Rox* unrelated to catabolism.

c External respiration, including aerobic microbial respiration, and extracellular O₂ consumption.



MIPart by Odra Noel



Figure 2. Respiratory states (ET, OXPHOS, LEAK) and corresponding rates (E, P, L)

Net OXPHOS-capacity, *P-L*, and excess capacity, *E-P*.

Table 1. Coupling states and residual oxygen consumption in mitochondrial preparations in relation to respiration- and phosphorylation-flux, *J_{ko}*, and *J_p*, and protonmotive force, Δp . Coupling states are established at kinetically-saturating concentrations of fuel substrates and O₂.

| State | <i>J_{ko}</i> | <i>J_p</i> | Δp | Inducing factors | Limiting factors |
|--------|--|----------------------|------------|--|--|
| LEAK | <i>L</i> ; low, cation leak-dependent respiration | 0 | max. | proton leak, slip, and cation cycling | <i>J_p</i> = 0: (1) without ADP, <i>L_s</i> ; (2) max. ATP/ADP ratio, <i>L_r</i> ; or (3) inhibition of the phosphorylation-pathway, <i>L_{only}</i> |
| OXPHOS | <i>P</i> ; high, ADP-stimulated respiration | max. | high | kinetically-saturating [ADP] and [P _i] | <i>J_p</i> , by phosphorylation-pathway; or <i>J_{ko}</i> , by ET-capacity |
| ET | <i>E</i> ; max., noncoupled respiration | 0 | low | optimal external uncoupler concentration for max. <i>J_{o,e}</i> | <i>J_{ko}</i> , by ET-capacity |
| ROX | <i>Rox</i> ; min., residual O ₂ consumption | 0 | 0 | <i>J_{o,leak}</i> in non-ET-pathway oxidation reactions | inhibition of all ET-pathways; or absence of fuel substrates |

Figure 3. Normalization of rate

A: Cell respiration is normalized for (1) the experimental **Sample** (flow per object, *N_o*, mass-specific flux, or cell-volume-specific flux); or (2) for methodological reasons for the **Chamber** volume.

B: Flow per cell [amol O₂ s⁻¹ cell⁻¹] is flux per chamber volume, *J_v* [nmol O₂ s⁻¹ L⁻¹], divided by cell concentration in the chamber, *N_{ce}*/V [cells L⁻¹], which is **Number** analysis. In **Structure** analysis, aerobic cell performance is mt-quality (mt-specific flux, e.g., per citrate synthase, CS) times mt-quantity, or mt-function times mt-structure.



MitoEAGLE
Join
COST Action CA15203

Funded by the Horizon 2020 Framework Programme of the European Union

www.mitoeagle.org/index.php/MitoEAGLE

COST Action CA15203 MitoEAGLE

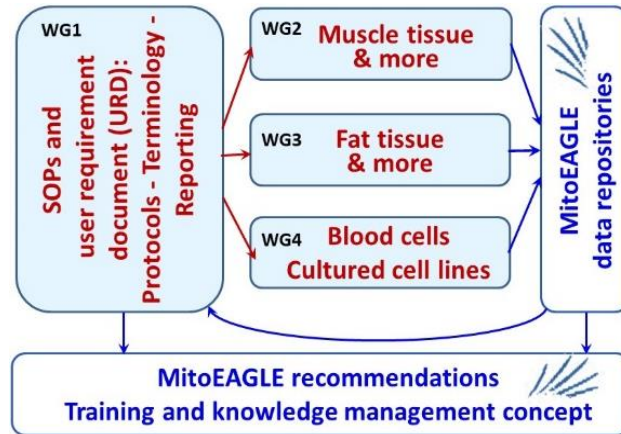
Evolution Age Gender
Lifestyle Environment



Mission of the global MitoEAGLE network

in collaboration with the Mitochondrial Physiology Society, MiPs

- Improve our knowledge on mitochondrial function in health and disease with regard to Evolution, Age, Gender, Lifestyle and Environment
- Interrelate studies across laboratories with the help of a MitoEAGLE data management system
- Provide standardized measures to link mitochondrial and physiological performance to understand the myriad of factors that play a role in mitochondrial physiology



Join the COST Action MitoEAGLE - contribute to the quality management network.



More information:
www.mitoeagle.org



Funded by the Horizon 2020 Framework Programme
of the European Union

